and B4 where the signs are reversed in **10** compared to the difference between the deprotonated and protonated nucleoside and nucleotide. This suggests that in addition to hydrogen bonding between B3 and an e side chain amide hydrogen another interaction may be occurring involving the top edge of the benzimidazole moiety. This additional interaction could be a hydrophobic interaction between the top edge of the benzimidazole moiety and the e side chain methylene groups, although we cannot rule out the possibility that dipolar shielding from the cobalt atom is responsible for this effect, as neither the exact geometry of the hydrogen-bonded species nor the magnetic anisotropy of the cobalt atom in any base-off cobalamin is known.

Attempts are currently in progress to evaluate the equilibrium constant for formation of the hydrogen-bonded base-off complex and thus to reinterpret the thermodynamics of the base-on/base-off reaction. These results will be reported in a subsequent communication.

Acknowledgment. This research was supported by the Robert A. Welch Foundation, Houston, Texas, Grant Y-749. The author is grateful to J. M. Hakimi and Y.-J. Huang for technical assistance. The author is also most grateful to M. F. Summers, L. G. Marzilli, and A. Bax for communicating results prior to their publication, and to D. W. Jacobsen for HPLC analyses.

Chlorophyll Model Compounds: Effects of Low Symmetry on the Resonance Raman Spectra and Normal Mode Descriptions of Nickel(II) Dihydroporphyrins

Nancy J. Boldt, Robert J. Donohoe, Robert R. Birge, and David F. Bocian*

Contribution from the Department of Chemistry, Carnegie Mellon University, Pittsburgh, Pennsylvania 15213. *Received September 26, 1986*

Abstract: Resonance Raman (RR) spectra are reported for a series of nickel(II) dihydroporphyrins with excitation in the B, Q_x, and Q_y absorption regions. The molecules include *trans*-octaethylchlorin, γ,δ-deuteriated *trans*-octaethylchlorin, 9-deoxomethylmesopyropheophorbide *a*, methylmesopyropheophorbide *a*, and methylpyropheophorbide *a*. These molecules represent a series in which the structural complexities of chlorophyll *a* (reduced pyrrole ring, isocyclic ring, 9-keto group, and 2-vinyl group) are systematically added to the basic tetrapyrrole structure. All of the observed in-plane chlorin skeletal modes and vibrations of the isocyclic ring and vinyl group are assigned. Assignments are then proposed for chlorophyll *a* based on analogy to those of the Ni(II) complexes. In addition to the spectral assignments, normal coordinate calculations are performed on the various nickel(II) dihydroporphyrins. These calculations indicate that the forms of the normal coordinates of the metallochlorins bear little resemblance to those of the parent metalloporphyrins. In the low-symmetry environment which characterizes the reduced pyrrole pigments, a number of the vibrations are localized in semicircles or quadrants of the macrocycle rather than being delocalized over the entire ring. This vibrational localization is due to geometrical changes in the π-bonded system which occur as a result of reduction of one of the pyrrole rings and addition of the isocyclic ring.

I. Introduction

Metallodihydroporphyrins (metallochlorins) are ubiquitous in nature, occurring in various chlorophyll pigments,[1] in the marine worm pigment, bonellin,[2] and in the green heme proteins, myeloperoxidase,[3,4] sulfmyoglobin,[5-7] sulfhemoglobin,[7b,8] and microbial hemes *d* and d_1.[3,9-12] The biological rationale for the presence of a prosthetic group which contains one reduced pyrrole ring (or two in the case of bacteriochlorophyll) is not presently understood. However, it is clear that modification of the basic tetrapyrrole structure significantly alters the photophysical, redox, and ligand binding properties of metallochlorin vs. metalloporphyrin systems.[13-16] The altered nature of these physical properties is presumably responsible for the evolutionary selection of the metallodihydroporphyrin moiety as the active unit in the protein.

Resonance Raman (RR) spectroscopy has proven to be an extremely useful probe of the vibrational and electronic structure of metalloporphyrins and heme proteins.[17-20] More recently, metallochlorins and chlorophyll have come under increased scrutiny by the RR technique.[3,4,6,21-27] The RR spectra of me-

(1) Svec, W. A. In *The Porphyrins*; Dolphin, D., Ed.; Academic Press: New York, 1978; Vol. V, pp 341-399.
(2) Ballantine, J. A.; Psaila, A. F.; Pelter, A.; Murray-Rust, P.; Ferrito, V.; Schembri, P.; Jaccarini, V. *J. Chem. Soc., Perkin Trans. 1* **1980**, 1080-1089.
(3) Sibbet, S. S.; Hurst, J. K. *Biochemistry* **1984**, *23*, 3007-3013.
(4) Babcock, G. T.; Ingle, R. T.; Oertling, W. A.; Davis, J. C.; Averill, B. A.; Hulse, C. L.; Stufkens, D. J.; Bolscher, B. G. J. M.; Wever, R. *Biochim. Biophys. Acta* **1985**, *828*, 58-66.
(5) Morell, D. B.; Chang, Y.; Clezy, P. S. *Biochim. Biophys. Acta* **1967**, *136*, 121-136.
(6) Andersson, L. A.; Loehr, T. M.; Lim, A. R.; Mauk, A. G. *J. Biol. Chem.* **1984**, *259*, 15340-15349.
(7) (a) Peisach, J.; Blumberg, W. E.; Adler, A. *Ann. N.Y. Acad. Sci.* **1973**, *206*, 310-327. (b) Berzofsky, J. A.; Peisach, J.; Blumberg, W. E. *J. Biol. Chem.* **1971**, *246*, 3367-3377.
(8) Brittain, T.; Greenwood, C.; Barber, D. *Biochim. Biophys. Acta* **1982**, *705*, 26-32.
(9) Lemberg, R.; Barrett, J. In *Cytochromes*; Academic Press: London, 1973; pp 233-245.
(10) Timkovich, R.; Cork, M. S.; Gennis, R. B.; Johnson, P. Y. *J. Am. Chem. Soc.* **1985**, *107*, 6060-6075.
(11) (a) Chang, C. K. *J. Biol. Chem.* **1985**, *260*, 9520-9522. (b) Chang, C. K.; Wu, W. *J. Biol. Chem.* **1986**, *261*, 8593-8596.
(12) Chang, C. K.; Barkigia, K. M.; Hanson, L. K.; Fajer, J. *J. Am. Chem. Soc.* **1986**, *108*, 1352-1354.
(13) (a) Scheer, H.; Inhoffen, H. H. In *The Porphyrins*; Dolphin, D., Ed.; Academic Press: New York, 1978; Vol. II, pp 45-90. (b) Weiss, C. In *The Porphyrins*; Dolphin, D., Ed.; Academic Press: New York, 1978; Vol. III, pp 211-223.
(14) Stolzenberg, A. M.; Strauss, S. H.; Holm, R. H. *J. Am. Chem. Soc.* **1981**, *103*, 4763-4778.
(15) Feng, D.; Ting, Y.-S.; Ryan, M. *Inorg. Chem.* **1985**, *24*, 612-617.
(16) Strauss, S. H.; Thompson, R. G. *J. Inorg. Biochem.* **1986**, *27*, 173-177.
(17) Johnson, B. B.; Peticolas, W. *Annu. Rev. Phys. Chem.* **1976**, *27*, 465-491.
(18) Spiro, T. G.; Stein, P. *Annu. Rev. Phys. Chem.* **1977**, *28*, 501-521.
(19) Felton, R. H.; Yu, N.-T. In *The Porphyrins*; Dolphin, D., Ed.; Academic Press: New York, 1978; Vol. II, pp 341-388.
(20) Spiro, T. G. In *Iron Porphyrins*; Lever, A. B. P., Gray, H. B., Eds.; Addison-Wesley: Reading, MA, 1982; Part II, pp 89-152.
(21) (a) Ozaki, Y.; Kitagawa, T.; Ogoshi, H. *Inorg. Chem.* **1979**, *18*, 1772-1776. (b) Ozaki, Y.; Iriyama, K.; Ogoshi, H.; Ochiai, T.; Kitagawa, T. *J. Phys. Chem.* **1986**, *90*, 6051-6112; (c) Ozaki, Y.; Iriyama, K.; Ogoshi, H.; Ochiai, T. Kitagawa, T. *Ibid.* **1986**, *90*, 6113-6118.
(22) Cotton, T. M.; Timkovich, R.; Cork, M. S. *FEBS Lett.* **1981**, *133*, 39-41.
(23) Ching, Y.; Ondrias, M. R.; Rousseau, D. L.; Muhoberac, B. B.; Wharton, D. C. *FEBS Lett.* **1982**, *138* 239-244.

0002-7863/87/1509-2284$01.50/0

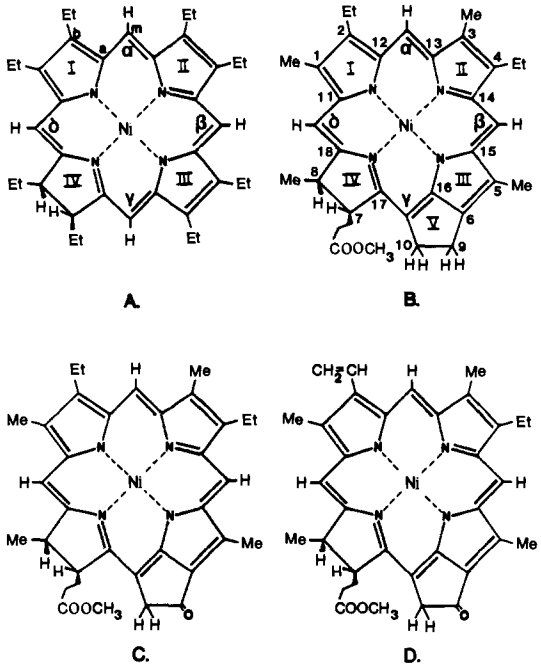

Figure 1. Structures and labeling scheme for the nickel(II) dihydroporphyrins: A, NiOEC; B, NiDMPPh; C, NiMPPh; D, NiPPh.

tallochlorins are more complex than those of metalloporphyrins because the reduced symmetry of the macrocycle results in RR activity for many more modes than in the symmetrical metalloporphyrins. The RR spectra of chlorophyll are more complex still due to the presence of an isocyclic ring which is added to the basic chlorin structure. Nevertheless, progress has been made toward identifying Raman bands which exhibit significantly different frequencies or intensity enhancements in metallochlorins vs. metalloporphyrins and, hence, can be used as general markers for the presence of a metallodihydroporphyrin prosthetic group.[24] In addition, assignments have been suggested for a number of the RR and IR bands of metallochlorins[24] and chlorophyll;[27a] however, these assignments are based primarily on the comparison of the spectra of these molecules with those of metalloporphyrins.[28] Implicit in the assignments is the assumption that the normal mode compositions are not significantly altered upon reduction of one of the pyrrole rings or addition of an isocyclic ring.

Although much progress has been made recently in the characterization of the vibrational spectra of metallochlorins and chlorophyll, there are still large deficiencies both in the number and types of complexes which have been examined and in the detailed interpretation of the spectral data. The acquisition of additional data is important for understanding the vibrational spectra of metallodihydroporphyrins in general but particularly crucial for the interpretation of chlorophyll spectra. In the latter system, the complexities introduced by the presence of the isocyclic ring, in addition to the reduced pyrrole, render the examination

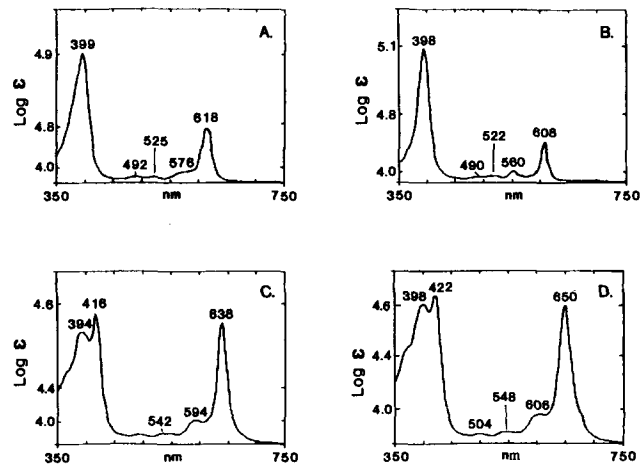

Figure 2. Electronic Absorption spectra of the nickel(II) dihydroporphyrins: A, NiOEC in $CHCl_3$; B, NiDMPPh in CH_2Cl_2; C, NiMPPh in CH_2Cl_2; D, NiPPh in CH_2Cl_2.

of structural intermediates mandatory. At this time, no such studies have appeared. The interpretation of the vibrational spectra of the metallochlorins and chlorophyll also requires that normal coordinate calculations be performed. The lack of spectral data has precluded such analyses even for simple model systems. Thus, no quantitative assessment of the effects of reduction of one of the pyrrole rings (or addition of an isocyclic ring) on the form of the vibrational modes is currently available.

In this paper we report a detailed RR study of the Ni(II) complexes of the series of dihydroporphyrins shown in Figure 1. These molecules include *trans*-octaethylchlorin (OEC), γ,δ-deuteriated OEC (OEC-$\gamma\delta$-d_2), 9-deoxomethylmesopyropheophorbide *a* (DMPPh), methylmesopyropheophorbide *a* (MPPh), and methylpyropheophorbide *a* (PPh). The molecules represent a series in which the structural complexities of chlorophyll *a* (reduced pyrrole ring, isocyclic ring, 9-keto group, and 2-vinyl group) are systematically added to the basic tetrapyrrole structure. Each of the structural modifications significantly influences the electronic properties of the system, as is evidenced by the electronic absorption spectra shown in Figure 2. Complexes with Ni(II), rather than Mg(II), were chosen for study for two reasons. First, the vibrational spectra and normal coordinate analysis of NiOEP (OEP = octaethylporphyrin) are the benchmark for the interpretation of the spectra of metalloporphyrins.[28] The scrutiny which has been given to NiOEP suggests that examination of nickel(II) dihydroporphyrins holds the greatest promise for accurate spectral characterization. Second, complexation of dihydroporphyrins with the open-shell Ni(II) ion completely quenches the fluorescence emission from the photophysically important, lowest energy $^1\pi\pi^*$ state.[24b] The inability to obtain red-excitation RR spectra of chlorophylls has severely hampered the characterization of the vibrational spectra of these photosynthetic pigments. RR spectra obtained with excitation into the lowest energy $^1\pi\pi^*$ states are essential for gaining a complete picture of the complicated vibrational structure of metallodihydroporphyrins, as has been demonstrated by Andersson et al.[24b,c] In addition to the spectral studies, we obtain normal mode descriptions for the various molecules by using the quantum chemistry force field (QCFF/PI) method of Warshel and Karplus.[29] These calculations provide new insights into the effects of low symmetry on the forms of the normal modes of reduced pyrrole pigments and reveal that previous vibrational characterizations, which are based on analogy to metalloporphyrins, are inappropriate. Together, the RR studies and normal coordinate calculations reported here allow us to propose a more detailed assignment for the vibrational spectrum of chlorophyll *a*.

The organization of this paper is as follows. First, we present the results of the RR study and summarize the assignments for

(24) (a) Andersson, L. A.; Loehr, T. M.; Chang, C. K.; Mauk, A. G. *J. Am. Chem. Soc.* **1985**, *107*, 182–191. (b) Andersson, L. A.; Loehr, T. M.; Sotiriou, C.; Wu, W.; Chang, C. K. *J. Am. Chem. Soc.* **1986**, *108*, 2908–2916. (c) Andersson, L. A.; Sotiriou, C.; Chang, C. K.; Loehr, T. M. *J. Am. Chem. Soc.*, in press.

(25) (a) Cotton, T. M.; van Duyne, R. P. *J. Am. Chem. Soc.* **1981**, *103*, 6020–6026. (b) Cotton, T. M.; Parks, K. D.; van Duyne, R. P. *J. Am. Chem. Soc.* **1980**, *102*, 6399–6407. (c) Cotton, T. M.; Van Duyne, R. P. *Biochem. Biophys. Res. Commun.* **1978**, *82*, 424–433.

(26) (a) Fujiwara, M.; Tasumi, M. *J. Phys. Chem.* **1986**, *90*, 250–255. (b) Fujiwara, M.; Tasumi, M. *Ibid.* **1986**, *90*, 5646–5650.

(27) (a) Lutz, M. In *Advances in Infrared and Raman Spectroscopy*; Clark, R. J. H., Hester, R. E., Eds.; John Wiley & Sons: New York, 1984; Vol. 11, pp 211–300. (b) Robert, B.; Lutz, M. *Biochemistry* **1986**, *25*, 2303–2309. (c) Lutz, M.; Hoff, A. L.; Brehanet, L. *Biochim. Biophys. Acta* **1982**, *679*, 331–341. (d) Lutz, M. *J. Raman Spectrosc.* **1974**, *2*, 497–516. (e) Lutz, M. *J. Biochem. Biophys. Res. Commun.* **1973**, *53*, 413–418.

(28) (a) Kitagawa, T.; Abe, M.; Ogoshi, H. *J. Chem. Phys.* **1978**, *69*, 4516–4525. (b) Abe, M.; Kitagawa, T.; Kyogku, Y. *Ibid.* **1978**, *69*, 4526–4534.

(29) Warshel, A.; Karplus, M. *J. Am. Chem. Soc.* **1975**, *94*, 5612–5625.

the vibrational modes of the metallodihydroporphyrins. Next we discuss the vibrational assignments and the influence of the isocyclic ring, keto group, and vinyl group on the spectra. We then examine the effects of low symmetry on the electronic and vibrational structures of the molecules. Finally, we comment on the possible influence of the normal mode structure on interchromophore interactions in aggregates of photosynthetic pigments.

II. Methods

A. Experimental Procedures. *trans*-OEC was prepared from OEP (Midcentury Chemicals, Posen, IL) according to the method of Whitlock et al.[30] Methyl pyropheophorbide *a* was prepared by refluxing methyl pheophorbide *a* for 1.5 h in collidine under N_2 in the dark.[31] Methyl pheophorbide *a* was isolated from spray-dried *Spirulina maxima* algae (Earthrise Company, San Rafael, CA) by the method of Smith et al.[31] NiOEC and NiPPh were prepared and purified by the method of Boucher and Katz[32] which was modified as follows. The free base was heated in a glacial acetic acid/methylene chloride (5/1) solution under N_2. A fourfold excess of nickel(II) acetate was added, and the solution was refluxed for 1 h. The metalated complex was extracted into benzene, washed with water, and dried over Na_2SO_4, and the solvent was removed. NiOEC was purified on a magnesium oxide (heavy) column with hexane/benzene (9/1) as the elutant. NiPPh was purified on an alumina column (Grade III) with a 1% propanol in benzene solution as the elutant. NiDMPPh and NiMPPh were synthesized and purified as the metalated complexes directly from NiPPh according to the method of Smith and Goff.[33] NiOEC-γ,δ-d_2 was prepared in a one-pot synthesis by adding nickel(II) acetate to the solution containing the deuteriated compound (prepared according to Smith[34]) and refluxing for an additional 20 min. The extent of deuteriation at the γ,δ-positions was determined to be greater than 90% by proton NMR.

The RR spectra were recorded on a computer-controlled Spex Industries 1403 double monochromator equipped with a thermoelectrically cooled Hamamatsu R928 photomultiplier tube and a photon-counting detection system. Excitation wavelengths were provided by a tunable dye laser (Coherent Radiation 590-03) utilizing the tuning range of Rhodamine 6G (Exciton Chemical Co.) and the discrete outputs of Ar ion (Coherent Radiation Innova 15UV) and Kr ion (Coherent Radiation K-2000) lasers. Unpolarized RR spectra were obtained of samples suspended in compressed pellets with a supporting medium of Na_2SO_4 (4–6 mg of sample/100 mg Na_2SO_4). The samples were spun to prevent photodecomposition. Solution samples (CS_2, CH_2Cl_2, and benzene) contained in sealed capillary tubes were used to collect polarization data. RR spectra were collected at 2-cm^{-1} intervals at a rate of 1 s/point. The incident powers were approximately 30, 70, and 50 mW for the B, Q_x, and Q_y absorption regions, respectively. The spectral slit width was 3 cm^{-1} for B and Q_x excitation and 6 cm^{-1} for Q_y excitation.

B. Normal Coordinate Calculations. The vibrational frequencies and normal mode descriptions of the nickel(II) dihydroporphyrins were calculated by using the QCFF/PI method.[29,35] This approach was chosen in lieu of conventional normal-mode analysis techniques because it does not require the estimation and refinement of a large number of force constants. The QCFF/PI approach has been used successfully by Warshel and co-workers to predict the vibrational frequencies, normal-mode descriptions and vibrational intensities (IR and RR) of metalloporphyrins[36] and other large, biological molecules such as retinal.[37,38] This computational procedure determines the ground- and excited-state potential surfaces based on an empirical σ-potential function and a semiempirical Pariser–Parr–Pople π-electron calculation which includes single excitation configuration interaction. An optimized geometry is produced in the course of the orbital energy minimization. The utility of the QCFF/PI approach is underscored by the fact that, to date, it has provided the only reliable description of the out-of-plane modes of metalloporphyrins.[36,39]

The vibrational calculations were initiated by computing the normal modes of NiOEP. Force constants which are not included in the program were taken from the literature[28b,36] or estimated.[40] The input geometry was that of planar NiOEP[41] with the C_b-ethyl substituents represented as 15 amu point masses.[28b] The QCFF/PI procedure was found to yield optimized geometries and vibrational frequencies in good agreement with the experiment.[42] Comparison of the normal mode descriptions predicted by the QCFF/PI calculation with those obtained by using conventional Urey–Bradley (Abe et al.[28b]) or valence bond (Gladkov and Solovyov[43]) force fields showed that the QCFF/PI approach yielded similar results. However, the exact forms of the potential energy distributions are different among all three calculations because the vibrational force fields are different from one another. In general, our calculated modes more closely resemble those reported by Abe et al., most probably because the C_b-ethyl groups are approximated as point masses in both calculations. The Soviet workers included the internal vibrations of these groups in their calculations. It should be noted that the identification of the E_u modes of NiOEP in the 1100–1300-cm^{-1} spectral region is the subject of some controsversy (cf. Kincaid et al.,[44] Abe et al.,[28b] and Gladkov and Solovyov[43c]). Our normal coordinate calculations do not aid in the resolution of this controversy because the frequencies of the IR bands which have been proposed for a specific mode by the various workers are not very different.

The extension of the calculations from NiOEP to the nickel(II) dihydroporphyrins proved to be straightforward. The force constants and the point-mass descriptions of the C_b substituents were retained while the input geometries were altered to include a trans configuration for ring IV and rough estimates of the positions of the additional atoms (reduced pyrrole hydrogens and ring V atoms). A comparison of the optimized geometries with the crystal structures of several metallodihydroporphyrins revealed many gratifying similarities.[45–49] Of particular note is the accurate

(30) Whitlock, H. W.; Hanaver, R.; Oester, M. Y.; Bower, B. K. *J. Am. Chem. Soc.* **1969**, *91*, 7485–7489.
(31) Smith, K. M.; Goff, D. A.; Simpson, D. J. *J. Am. Chem. Soc.* **1985**, *107*, 4946–4954.
(32) Boucher, L. J.; Katz, J. J. *J. Am. Chem. Soc.* **1967**, *89*, 4703–4708.
(33) Smith, K. M.; Goff, D. A. *J. Am. Chem. Soc.* **1985**, *107*, 4954–4965.
(34) Fuhrhop, J. P.; Smith, K. M. In *Porphyrins and Metalloporphyrins*; Smith, K. M., Ed.; Elsevier: Amsterdam, 1975; p 817.
(35) Warshel, A.; Levitt, M. *Quantum Chemistry Program Exchange*, No. 247, Indiana University, 1974.
(36) Warshel, A.; Lappicirella, A. *J. Am. Chem. Soc.* **1981**, *103*, 4664–4673.
(37) Warshel, A.; Dauber, P. *J. Chem. Phys.* **1977**, *66*, 5477–5488.
(38) Warshel, A. *Annu. Rev. Biophys. Bioeng.* **1977**, *6*, 273–300.
(39) Choi, S.; Spiro, T. G. *J. Am. Chem. Soc.* **1983**, *105*, 3683–3692.
(40) Estimated force constants (in order of required input): C_b substituent bond stretch parameters: 110 kcal/mol-Å^2, 1.5 Å, 88 kcal/mol. Nitrogen–metal dihedral constants: 0.7 kcal/mol, 0.0 kcal/mol-rad^2, 0.0 kcal/mol. Several program changes were required in order to accommodate the four-coordinate metal center. In order to provide for separate identification of the 180° and 90° N–M–N angles, it was necessary to assign two different atom labels for the pyrrole nitrogens. The identification of dihedral angles (subroutine PHIP) had to be altered to prevent inclusion of torsions involving colinear bonds.
(41) Scheidt, W. R. In *The Porphyrins*; Dolphin, D.; Ed.; Academic Press: New York, 1978; Vol. III, pp 463–511.
(42) The relative bond lengths of the macrocycle were calculated correctly for NiOEP, but the core size was too large (M–N = 2.06 Å). Adjustments of some force constants improved the calculated core size and frequencies but did not affect the eigenvectors. The calculated frequencies (cm^{-1}) for the skeletal motions of NiOEP above 1000 cm^{-1} are as follows: A_{1g} 1585 (ν_2), 1477 (ν_3), 1377 (ν_4), 1033 (ν_5); B_{1g} 1618 (ν_{10}), 1542 (ν_{11}), 1326 (ν_{12}), 1256 (ν_{13}), 1061 (ν_{14}); A_{2g} 1599 (ν_{19}), 1477 (ν_{20}), 1315 (ν_{21}), 1078 (ν_{22}), 1034 (ν_{23}); B_{2g} 1528 (ν_{28}), 1486 (ν_{29}), 1137 (ν_{30}), 1051 (ν_{31}); E_u 1587 (ν_{37}), 1567 (ν_{38}), 1499 (ν_{39}), 1476 (ν_{40}), 1353 (ν_{41}), 1292 (ν_{42}), 1087 (ν_{43}), 1076 (ν_{44}), 1005 (ν_{45}).
(43) (a) Gladkov, L. L.; Solovyov, K. N. *Spectrochim. Acta* **1985**, *41A*, 1437–1442. (b) Gladkov, L. L.; Solovyov, K. N. *Ibid.* **1985**, *41A*, 1443–1448. (c) Gladkov, L. L.; Solovyov, K. N. *Ibid.* **1986**, *42A*, 1–10.
(44) Kincaid, J. R.; Urban, M. W.; Watanabe, T.; Nakamoto, K. *J. Phys. Chem.* **1983**, *87*, 3096–3101.
(45) Spaulding, L. D.; Andrews, L. C.; Williams, G. J. B. *J. Am. Chem. Soc.* **1977**, *99*, 6918–6923.
(46) Gallucci, J. C.; Swepston, P. N.; Ibers, J. A. *Acta Crystallogr., Sect. B: Struct. Crystallogr. Cryst. Chem.* **1982**, *38B*, 2134–2139.
(47) (a) Strauss, S. H.; Silver, M. E.; Ibers, J. A. *J. Am. Chem. Soc.* **1983**, *105*, 4108–4109. (b) Strauss, S. H.; Silver, M. E.; Long, K. M.; Thompson, R. G.; Hudgens, R. A.; Spartalian, K.; Ibers, J. A. *J. Am. Chem. Soc.* **1985**, *107*, 4207–4215.

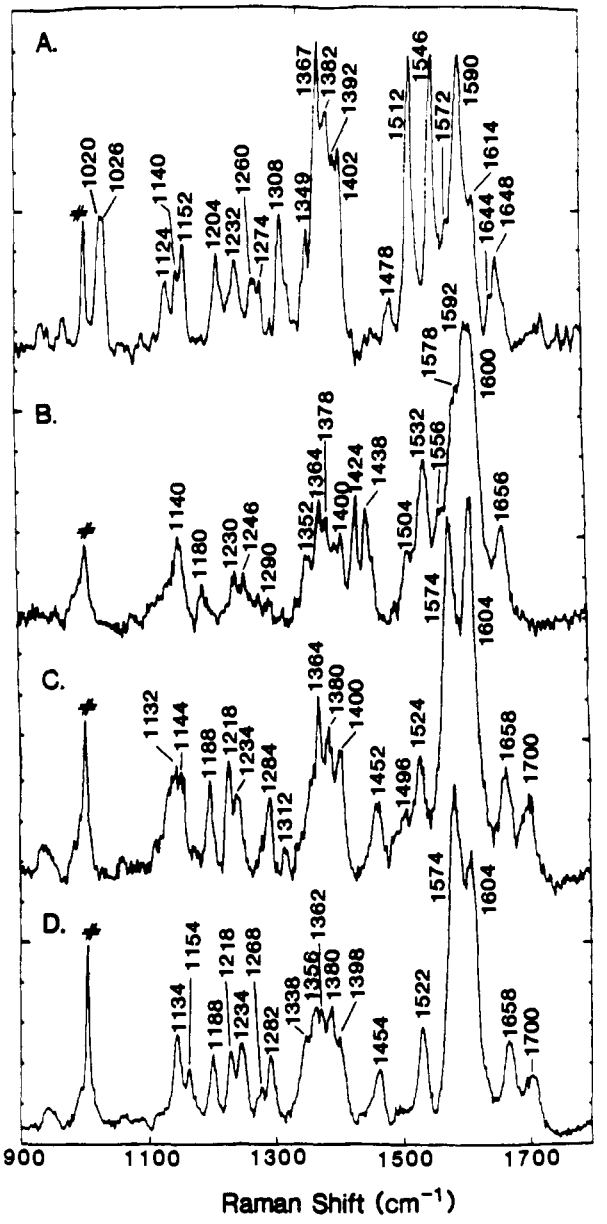

Figure 3. High-frequency region of the RR spectra of the nickel(II) dihydroporphyrins obtained with B-state excitation (λ_{ex} = 4067 Å): A, NiOEC; B, NiDMPPh; C, NiMPPh; D, NiPPh. The spectra are of solid samples in Na_2SO_4 pellets, and the internal standard is indicated by the symbol #.

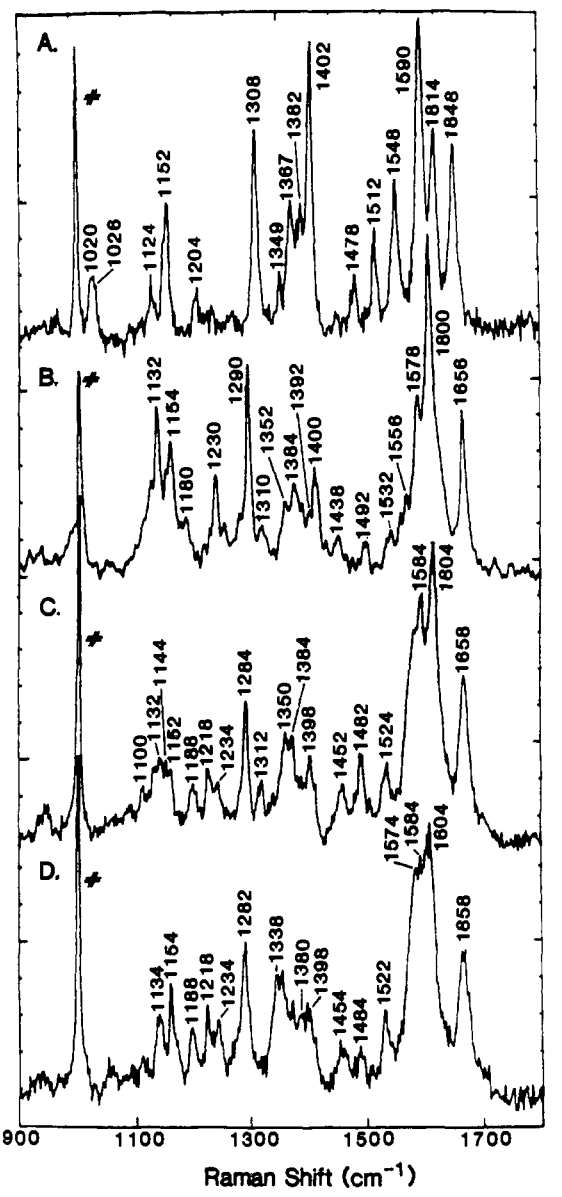

Figure 4. High-frequency region of the RR spectra of the nickel(II) dihydroporphyrins obtained with Q_x-state excitation: A, NiOEC (λ_{ex} = 4880 Å); B, NiDMPPh (λ_{ex} = 5287 Å); C, NiMPPh (λ_{ex} = 4880 Å); D, NiPPh (λ_{ex} = 5017 Å). The spectra are of solid samples in Na_2SO_4 pellets, and the internal standard is indicated by the symbol #.

reproduction of the alternating C_aC_m bond length pattern of metallo-OEC complexes (short–long–short–long, beginning from the reduced pyrrole). The calculation does not predict as large a degree of nonplanarity as is observed for nickel(II) dihydroporphyrins;[45,46] however, the degree of out-of-plane distortion of the core does not significantly affect the calculated vibrational frequencies and eigenvectors for modes above 1000 cm^{-1}. On the other hand, nonplanarity does alter the normal mode descriptions of low-frequency vibrations because of mixing of out-of-plane and low-frequency in-plane motions.

Subsequent to the initial calculations for NiOEP and the various nickel(II) dihydroporphyrins, attempts were made to improve the fits of the calculated and observed frequencies by allowing the σ-potential constants for the different types of CC bonds to be adjusted individually. This required substantial modification of the basic QCFF/PI program. It was found that, while the fit of the calculated vibrational frequencies could be improved for all the molecules, no significant changes occurred in the forms of the computed normal coordinates. This is not surprising because a change as large as 50 cm^{-1} in the frequency of a mode above 1000 cm^{-1} represents only a 3–5% change in the total energy. As a consequence, all the calculated vibrational frequencies and mode descriptions reported here were obtained by using the minimal force field.

III. Results

High-frequency RR spectra of the Ni(II) complexes of OEC, DMPPh, MPPh, and PPh obtained with excitation in the B, Q_x, and Q_y absorption bands are shown in Figures 3, 4, and 5, respectively. The exact excitation wavelengths are given in the figure legends. The corresponding low-frequency RR spectra are shown in Figures 6, 7, and 8, respectively. RR spectra were also recorded (not shown) at other excitation wavelengths in the Q-band region in order to facilitate the identification of RR bands. The RR spectrum of NiOEC has been reported previously by Ozaki et al.;[21] however, these workers used only a single excitation wavelength in the Q_x region. The Q_x region spectrum we obtained is nearly identical, although some differences in the RR frequencies and

(48) Fisher, M. S.; Templeton, D. H.; Zalkin, A.; Calvin, M. *J. Am. Chem. Soc.* **1972**, *94*, 3613–3619.
(49) Chow, H.-C.; Serlin, R.; Strouse, C. E. *J. Am. Chem. Soc.* **1975**, *97*, 7230–7237.

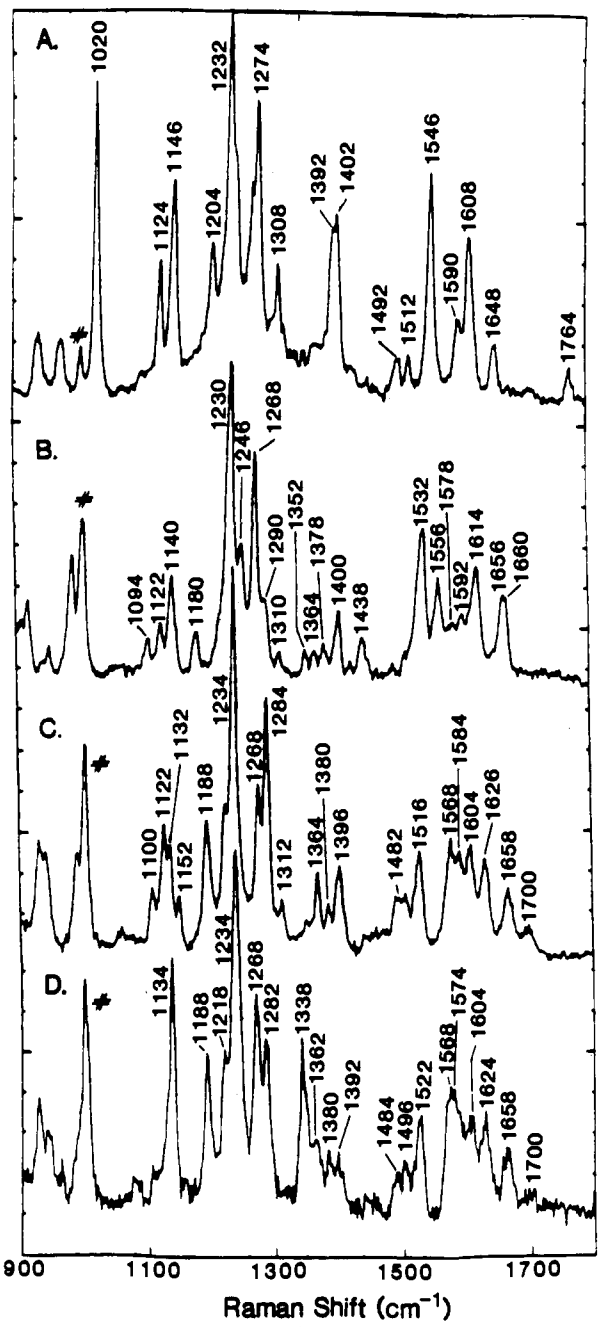

Figure 5. High-frequency region of the RR spectra of the nickel(II) dihydroporphyrins obtained with Q_y-state excitation: A, NiOEC (λ_{ex} = 5982 Å); B, NiDMPPh (λ_{ex} = 5982 Å); C, NiMPPh (λ_{ex} = 6471 Å); D, NiPPh (λ_{ex} = 6471 Å). The spectra are of solid samples in Na_2SO_4 pellets, and the internal standard is indicated by the symbol #.

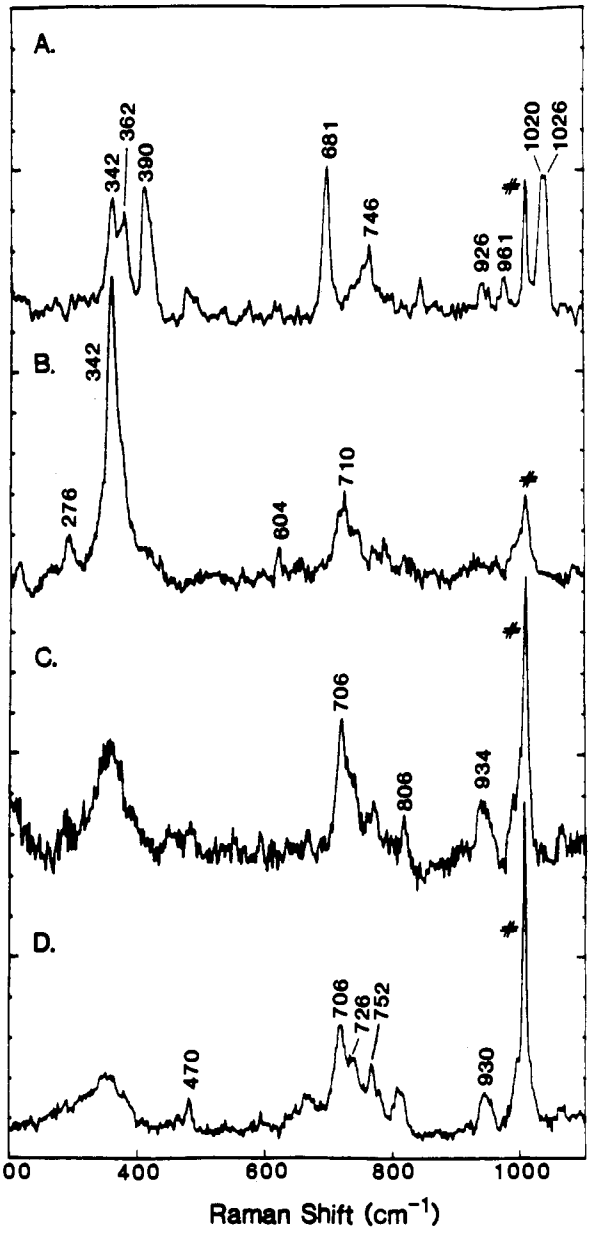

Figure 6. Low-frequency region of the RR spectra of the nickel(II) dihydroporphyrins obtained with B-state excitation (λ_{ex} = 4067 Å): A, NiOEC; B, NiDMPPh; C, NiMPPh; D, NiPPh. The spectra are of solid samples in Na_2SO_4 pellets, and the internal standard is indicated by the symbol #.

intensities can be noted between our spectra shown in Figures 4 and 7 (pellet samples) and those reported previously (solution samples). In general, the frequencies observed for the RR bands of solid samples of NiOEC and the other nickel(II) dihydroporphyrins were within 3 cm^{-1} of those observed for solution samples. The B-state excitation RR spectrum of solid samples of nickel(II) pheophorbide *a* has been reported by Fujiwara and Tasumi.[26b] This molecule contains a carbomethoxy group at the C_{10} position of ring V whereas NiPPh contains a hydrogen atom; however, the frequencies observed for the two complexes are similar.

The RR spectrum of NiOEC exhibits anomalously polarized (ap) bands in addition to the polarized (p) and depolarized (dp) bands expected for a molecule described by a low-symmetry point group (C_2). The depolarization ratios for the ap modes are in the range $\rho \sim 1.0$–1.2 while those of the p modes are $\rho \sim 0.33$. Polarized bands dominate the NiOEC RR spectra obtained with B and Q_y excitation, as has been observed for other metallochlorins,[24] while ap and dp modes dominate the spectrum obtained with Q_x excitation. However, comparison of the intensities of certain of the ap (1590 and 1308 cm^{-1}) and dp (1402 cm^{-1}) modes to the intensity of the internal standard reveals that the absolute intensity enhancements of these modes are approximately the same with Q_x and Q_y excitations (cf. Figures 4 and 5). It is also important to note that these ap and dp modes are clearly observed with B-state excitation (Figure 3). This observation indicates that the resonance enhancement mechanisms for the non-totally symmetric modes of metallochlorins are distinctly different from those of metalloporphyrins. In the case of NiDMPPh, NiMPPh, and NiPPh, all RR bands appear to be polarized with ρ values ranging from 0.3 to 0.6 depending on the excitation wavelength.

The observed and calculated frequencies and normal mode descriptions for the fundamental in-plane skeletal modes of NiOEC, NiDMPPh, and NiMPPh are listed in Tables I, II, and III, respectively. The polarizations of the RR bands of NiOEC are given in Table I. The observed frequencies for NiPPh are included in Table III. This latter complex differs from NiMPPh

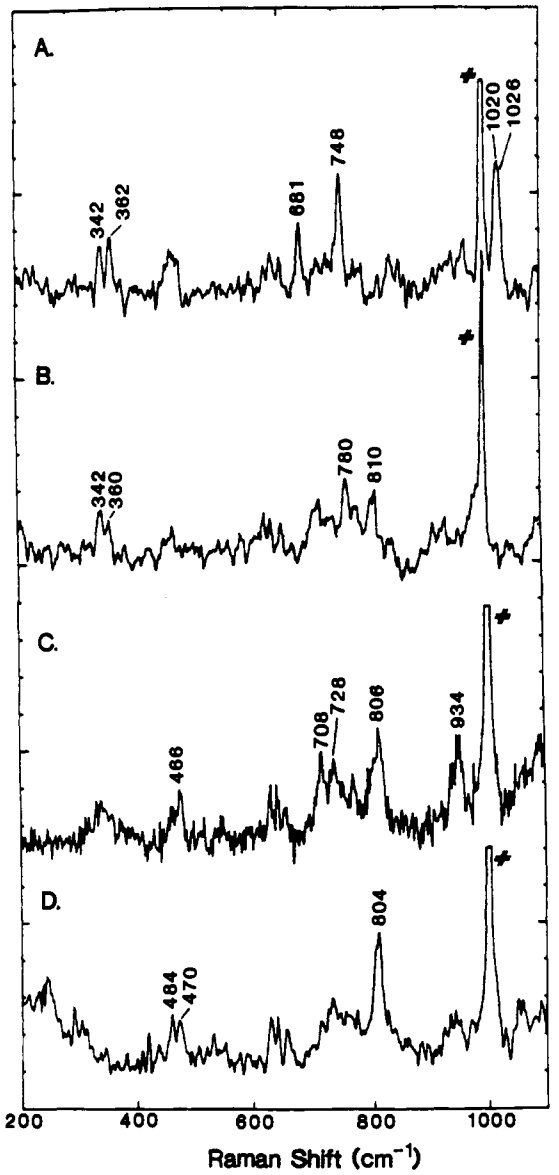

Figure 7. Low-frequency region of the RR spectra of the nickel(II) dihydroporphyrins obtained with Q_x-excitation state: A, NiOEC (λ_{ex} = 4880 Å); B, NiDMPPh (λ_{ex} = 5287 Å); C, NiMPPh (λ_{ex} = 4880 Å); D, NiPPh (λ_{ex} = 5017 Å). The spectra are of solid samples in Na_2SO_4 pellets, and the internal standard is indicated by the symbol #.

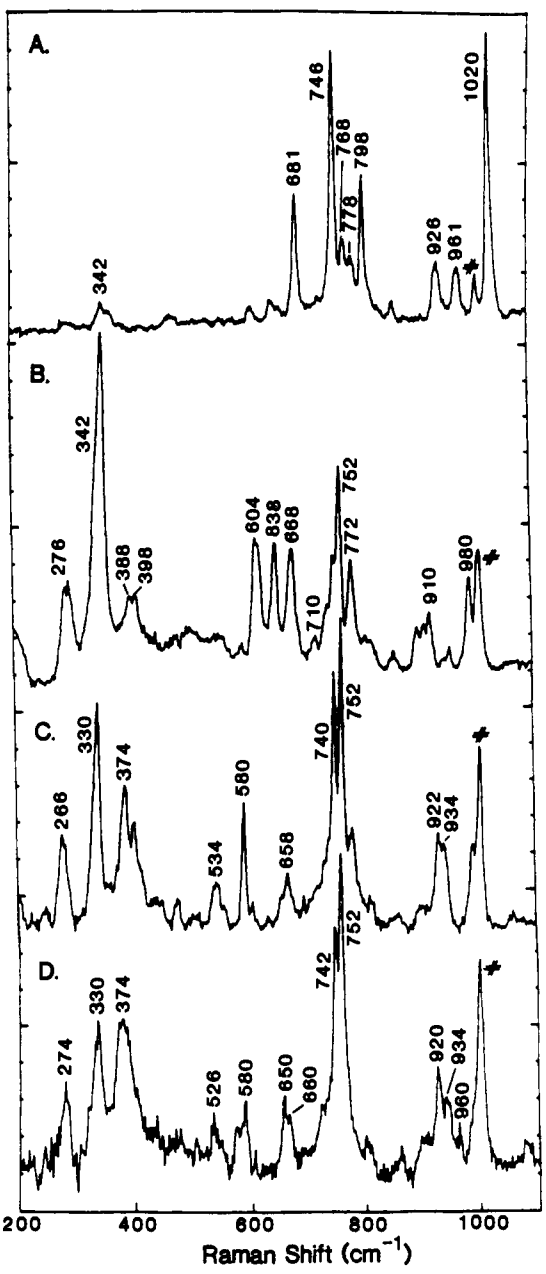

Figure 8. Low-frequency region of the RR spectra of the nickel(II) dihydroporphyrins obtained with Q_y-state excitation: A, NiOEC (λ_{ex} = 5982 Å); B, NiDMPPh (λ_{ex} = 5982 Å); C, NiMPPh (λ_{ex} = 6471 Å); D, NiPPh (λ_{ex} = 6471 Å). The spectra are of solid samples in Na_2SO_4 pellets, and the internal standard is indicated by the symbol #.

only in the substitution of a vinyl group for an ethyl group at the 2-position of the macrocycle (See Figure 1). This substituent change does not alter the form of the calculated normal coordinates because the C_b substituents are treated as point masses in the calculation (See Section II. B.). All observed and calculated fundamental modes with frequencies above 950 cm^{-1} are included in the tables. Below 950 cm^{-1} only those observed bands which can be assigned with reasonable certainty are listed. For the other low-frequency modes, the correlation of the experimental data with the calculations is uncertain due to the added complexity introduced into this region by the contribution of out-of-plane modes.

The relationship of the calculated normal modes of NiOEC to the normal modes of NiOEP is given in Table I. The labeling scheme for the NiOEP modes is that of Abe et al.[28b] As is evident from the table, few of the high-frequency modes of NiOEC can be directly correlated with a single NiOEP mode. In particular, vibrations which are exclusively Raman-active (A_{1g}, A_{2g}, B_{1g}, and B_{2g}) and those which are exclusively IR-active (E_u) in the high-symmetry porphyrin (D_{4h}) are extensively mixed in the low-symmetry chlorin (C_2). A few low-frequency vibrations of NiOEC do have calculated descriptions which are similar to those of the analogous modes of NiOEP;[28b] therefore, a one-to-one correlation is appropriate. In the case of the molecules containing the isocyclic ring, the further reduction in symmetry (C_1) precludes any meaningful description of the normal modes of the ring skeleton in terms of those of NiOEP. However, it is possible to relate the modes of the five-ring molecules to those of NiOEC and these relationships are given in Tables II and III.

Assignments for the more prominent combination and overtone bands of all the molecules are given in Table IV. Most of the modes listed in the table have analogues in the RR spectra of NiOEP and are derived from low-frequency fundamentals.[28] In order to facilitate comparison with NiOEP, the mode-labeling scheme of Abe et al. has been retained for the nonfundamentals of the nickel(II) dihydroporphyrins. In all cases the combinations and overtones of the dihydroporphyrins involve fundamentals that occur at nearly the same frequency as in NiOEP. Other bands which are probably due to nonfundamental vibrations are observed in the RR spectra of the reduced pyrrole systems; however, these bands cannot be assigned with any certainty.

Table I. Observed (RR) and Calculated Frequencies (cm^{-1}) of the Fundamental In-Plane Skeletal Modes for NiOEC

no.	sym	obsd[a]	calcd	assignment[b]	relation to NiOEP mode(s)[c]
1	A	1648 (p)	1649	νC_aC_m (γ, δ)	ν_{10}, ν_{37a}
2	B	1644 (ap)	1637	νC_aC_m (γ, δ)	ν_{37b}, ν_{19}
3	A	1614 (p)	1618	νC_aC_m (α, β)	ν_{37a}, ν_{10}
4	A	1608 (p)	1561	νC_bC_b (I, III)	ν_2, ν_{38a}, ν_{11}
5	B	1590 (ap)	1607	νC_aC_m (α, β)	ν_{19}, ν_{37b}
6	B	1572	1557	νC_bC_b (I, III)	ν_{38b}
7	A	1546 (p)	1532	νC_bC_b (II), νC_aC_m (α, β)	ν_{11}, ν_{38a}, ν_2
8	B		1540	νC_aC_b (II), νC_aC_b (I, III)	ν_{40b}
9	A	1512 (p)	1489	νC_aC_m (α, β, γ, δ), νC_aC_b (I, II, III)	ν_3, ν_{39a}
10	A	1492	1498	νC_aC_b (I, II, III)	ν_{40a}
11	B	1478 (dp)	1506	νC_aC_m (α, β, γ, δ), νC_aN (I, III)	ν_{28}
12	A		1480	νC_aC_m (γ, δ), νC_bC_b (I, II, III)	ν_{39a}, ν_3
13	B		1464	νC_aC_m (α, β), νC_aC_b (I, III), νC_bC_b (I, III)	ν_{39b}
14	B	1402 (dp)	1489	νC_aC_b (I, II, III), νC_aN (I, III, IV)	ν_{29}
15	B	1392 (ap)	1376	νC_aN (I, III, IV), νC_aC_b (I, III)	ν_{20}, ν_{41b}
16	A	1382 (p)	1398	νC_aN (I, III, IV), νC_bC_b (I, II, III)	ν_4, ν_{41a}
17	A	1367 (p)	1339	νC_aN (I, II, III, IV), νC_bC_b (I, II, III)	ν_{41a}, ν_4
18	A	1349	1315	νC_aN (I, II, III), νC_bC_b (II)	ν_{12}, ν_{41a}
19	B	1318 (sh)	1338	νC_aN (I, III, IV), δC_mH (γ, δ)	ν_{41b}, ν_{20}
20	B	1308 (ap)	1301	δC_mH (α, β), νC_aC_b (I, III)	ν_{21}, ν_{42b}
21	A	1274 (p)	1286	δC_mH (α, β), νC_aC_b (I, III)	ν_{13}, ν_{42a}
22	A	1232 (p)	1237	δC_bH (IV), δC_mH (γ, δ)	
23	B		1227	δC_bH (IV), δC_mH (γ, δ)	
24	A		1224	δC_mH (γ, δ), γC_bH (IV)	ν_{42a}, ν_{13}
25	A	1204 (p)	1171	δC_bH (IV), δC_aNC_a (IV)	
26	B		1200	γC_bH (IV)	
27	B	1152 (dp)	1147	νC_bEt (I, II, III), νC_aN	ν_{30}
28	A	1146 (p)	1082	νC_bEt (I, II, III), νC_aN (I, III)	ν_{43a}
29	B	1124 (ap)	1083	νC_bEt (I, II, III), δC_mC_aN (IV)	ν_{43b}, ν_{22}
30	B		1107	νC_aN (I, II, III, IV), δC_mH (γ, δ)	ν_{22}, ν_{43b}
31	A		1072	νC_bEt (II), νC_aN (I, II, III)	ν_{44a}, ν_{14}
32	B		1069	νC_bEt (II), νC_aN (I, II, III)	ν_{44b}, ν_{31}
33	B		1056	$\delta C_aC_mC_a$ (α, β, γ, δ), νC_aN (I, III)	ν_{31}, ν_{44b}
34	A		1049	νC_bEt (I, III), δC_mC_aN (α, β)	ν_{14}, ν_{44a}
35	B	1026 (ap)	1016	νC_aC_b (IV), νC_bEt (I, II, III)	ν_{23}, ν_{45b}
36	A	1020 (p)	1019	νC_bEt (I, II, III), δC_aNC_a (II)	ν_5, ν_{45a}
37	B		1004	νC_bEt (I, III), δC_mC_aN (α, β)	ν_{45b}, ν_{31}
38	A		967	νC_bC_b (IV)	ν_{38a}, ν_2, ν_{11}
				Prominent Modes below 950 cm^{-1} [d]	
39	A	926 (p)	881	δC_bC_bEt (I, II, III)	ν_{46a}
40	A	798 (p)	746	δC_bC_bEt (I, II, III)	ν_6
41	B	778	819	δC_aC_bEt (IV), νC_bEt (IV)	ν_{32}
42	B	766	790	δC_aC_bEt (I, III)	ν_{24}
43	A	746 (p)	706	δC_aC_bEt (I, II, III)	ν_{16}
44	A	681 (p)	651	$\delta C_aC_mC_a$ (α, β, γ, δ), νC_aC_b (I, II, III, IV)	ν_7
45	A	342 (p)	354	δC_aC_bEt (I, II, III, IV), νC_aC_m (γ, δ)	ν_8

[a] Abbreviations: p, polarized; ap, anomalously polarized; dp, depolarized; sh, shoulder. [b] Mode descriptors are as follows: ν = stretch, δ = in-plane deformation, and γ = out-of-plane deformation. C_a, C_b, C_m and the characters in parentheses refer to the macrocycle positions shown in Figure 1. [c] NiOEP mode descriptions are those given in ref 28b. [d] Other modes are observed below 950 cm^{-1}; however, the correlation of observed and calculated frequencies is very uncertain due to the high density of calculated modes.

The high-frequency RR spectra of NiOEC and NiOEC-γ,δ-d_2 obtained with Q_x and Q_y excitation are shown in Figure 9. Deuteriation shifts and new bands which appear upon deuteriation are indicated in the figure. RR spectra of the deuteriated complex were also obtained (not shown) by using B state excitation. Although RR spectra of NiOEC-γ,δ-d_2 have not been previously reported, Ozaki et al.[21] have obtained Q_x excitation spectra of the analogous Cu(II) complex. The spectral changes which occur upon deuteriation of the Ni(II) and Cu(II) complexes are similar. The modes of NiOEC which are substantially altered in composition upon deuteriation are listed in Table V. For these modes the normal coordinate calculations indicate that it is not appropriate to make a one-to-one correlation with modes of the deuteriated complex (See Section IV.A.1.c). Consequently, specific deuteriation shifts are not indicated for these modes in Figure 9. In cases where an unobserved mode of NiOEC is predicted to contribute substantially to an observed mode of NiOEC-γ,δ-d_2, the calculated frequency is given in the table.

The general features observed in the RR spectra of all the nickel(II) dihydroporphyrins are similar to those reported previously by Andersson et al.,[24] Ozaki et al.,[21] and Fujiwara and Tasumi.[26] These features include an increase in the total number of RR bands, an increase in the total number of polarized RR bands, and the occurrence of polarized bands with both B and Q_y state excitation. Nevertheless, the correlation of the RR bands of the nickel(II) dihydroporphyrins examined here with those of the various metallochlorins studied previously is not straightforward. Many of the molecules examined by other workers contain metal ions and/or β-pyrrole substituents different from those of the systems examined here. Changing the metal ion primarily effects the vibrational frequencies,[18-20,50-52] while changing the type and position of the β-pyrrole substituents primarily influences the RR intensity enhancements and polarizations.[53,54] These structural changes render the identification of analogous RR bands

(50) Spiro, T. G.; Strekas, T. C. *J. Am. Chem. Soc.* **1974**, *96*, 338-345.
(51) Spaulding, L. D.; Chang, C. C.; Yu, N.-T.; Felton, R. H. *J. Am. Chem. Soc.* **1975**, *97*, 2517-2525.
(52) Spiro, T. G.; Strong, J. D.; Stein, P. *J. Am. Chem. Soc.* **1979**, *101*, 2648-2655.
(53) Choi, S.; Lee, J. J.; Yei, Y. H.; Spiro, T. G. *J. Am. Chem. Soc.* **1983**, *105*, 3692-3707.
(54) (a) Willems, D. L.; Bocian, D. F. *J. Am. Chem. Soc.* **1984**, *106*, 880-890. (b) Willems, D. L.; Bocian, D. F. *J. Phys. Chem.* **1985**, *89*, 234-239.

Table II. Observed (RR) and Calculated Frequencies (cm^{-1}) of the Fundamental In-Plane Skeletal Modes for NiDMPPh

no.	obsd	calcd	assignment[a]	corresponding NiOEC modes[b]
1	1660	1688	νC_aC_m (γ)	1, 2
2	1656	1638	νC_aC_m (δ)	1, 2
3		1623	νC_bC_b (III), νC_aC_m (β)	4, 6
4	1614	1615	νC_aC_m (β), νC_aN (III)	3, 5, 11
5	1600	1570	νC_bC_b (I), νC_aC_m (α)	4, 6
6	1592	1608	νC_aC_m (α), νC_aC_b (II)	3, 5
7	1578	1585	νC_aC_b (III), νC_aC_b (II)	14
8		1555	νC_aC_b (II)	5, 8
9	1556	1540	νC_bC_b (II), νC_bC_b (I)	7
10	1532	1520	νC_aC_m (γ), νC_bC_b (III)	10, 12
11	1504	1510	νC_aC_b (I)	10, 12
12	1492	1488	νC_aC_b (I), νC_aC_m (δ)	9
13		1467	νC_aC_m (α, β)	13
14	1438	1452	γCH_2 (V-9) (scissors)	
15	1424	1444	γCH_2 (V-10) (scissors)	
16	1400	1489	νC_aC_b (II), νC_aC_m (α)	10
17	1392	1382	νC_aC_b (III), νC_aN (III)	15
18	1378	1402	νC_aN (IV), νC_aN (I, III)	16
19	1364	1337	νC_aN (I)	15, 17
20	1352	1305	νC_aN (II), νC_aC_b (III)	18
21	1310	1325	νC_aN (IV), νC_aN (II, III)	17
22	1290	1298	δC_mH (α, β), νC_aN (II)	20
23	1268	1280	δC_mH (α, β)	21
24		1246	δCH_2 (V-10) (wag), δCH_2 (V-9) (wag)	
25	1230	1228	δC_bH (IV), δC_mH (δ)	22, 23
26		1221	γC_bH (IV)	24
27		1206	γC_bH (IV), δC_mH (δ), νC_aC_b (I, IV)	24
28	1200 (sh)	1171	δC_bH (IV), νC_aN (IV), δC_mH (δ)	25, 30
29		1196	δCH_2 (V-9) (twist), δCH_2 (V-10) (twist)	
30	1180	1192	νC_mC_{10} (V), γC_bH (IV), νC_aN (III)	25
31	1154	1153	νC_aN (III, IV), δCH_2 (V) (wag)	27
32		1143	νC_aN (IV), νC_mC_{10} (V), $\delta C_aC_mC_a$ (δ)	30
33	1140	1085	δC_mC_aN (I, II, III), νC_bS	31
34	1132	1140	δCH_2 (V) (twist), $\delta C_aC_mC_a$ (α, β)	
35	1122	1100	νC_bS, δCH_2 (V) (wag)	29
36	1094	1068	νC_aN (I, III), δC_mH(δ), νC_aC_b (IV)	30, 31
37		1066	νC_aN (I, II), δC_mH (α)	32
38		1056	δC_mC_aN (I, II), νC_bS	31, 34
39		1051	νC_aN (II, III), νC_bS	34
40		1028	$\delta C_mC_aC_b$ (I, II, IV), νC_bS	35
41		1018	δC_mC_aN (I, II, III), νC_bS	
42		1005	νC_aN (III), δC_mC_aN (I, II), νC_9C_{10} (V)	37
43		970	νC_bC_b (IV)	38
			Prominent Modes below 950 cm^{-1} [c]	
44	772	805	νC_bS, $\delta C_aC_bC_b$ (IV)	
45	752	717	δC_aC_bS	41
46	668	648	$\delta C_aC_mC_a$ (α, β, δ)	44
47	342	360	δC_aC_bS	45

[a] S = C_b substituent. For explanation of other abbreviations and descriptors see Table I and Figure 1. [b] The modes of NiOEC which contain similar vibrational motions. Numbers refer to Table I. [c] Other modes are observed below 950 cm^{-1}; however, the correlation of observed and calculated frequencies is very uncertain due to the high density of calculated modes.

of different metallodihydroporphyrins difficult in many cases. On the other hand, comparison of the RR spectra of NiPPh with those reported for chlorophyll *a* by Lutz and co-workers reveals that the intensity enhancement patterns in the high-frequency regions (above 1350 cm^{-1}) are quite similar. In the mid-frequency region (1000–1350 cm^{-1}), both complexes exhibit similar RR frequencies and intensity enhancement patterns. Although NiPPh and chlorophyll *a* differ in the type of metal ion and the substituent group at the C_{10} position of ring V, the spectral similarities allow a direct correlation of most of the high- and mid-frequency skeletal modes. The vibrational assignments we propose for chlorophyll *a* are included in Table III.

IV. Discussion.

A. Vibrational Assignments. The vibrational assignments for the nickel(II) dihydroporphyrins were determined in a stepwise and concerted fashion. To begin, the observed RR spectra and calculated normal modes of NiOEC were compared with those of NiOEP.[28,43c] The polarization characteristics and intensity enhancement patterns of the RR bands of NiOEC proved extremely useful in the correlation of the spectra for the two complexes. In particular, most non-totally symmetric fundamentals of NiOEC which are observed at frequencies similar to those of A_{2g} fundamentals of NiOEP exhibit anomalous polarization (see Figure 4 and Table I). Also, most symmetric fundamentals of the chlorin which are observed at frequencies similar to those of B_{1g} fundamentals of the porphyrin are primarily enhanced with Q_y region excitation, while those which are observed at frequencies similar to those of A_{1g} fundamentals are primarily enhanced with B-state excitation (see Figures 3 and 5 and Table I). The 38 modes of NiOEC with calculated frequencies above 950 cm^{-1} were plotted and examined in detail in order to determine their relationship to the modes of NiOEP. The comparison of the eigenvectors of the two complexes resulted in the correlations listed in the last column of Table I, which indicate the extent of redistribution of the vibrational eigenvectors in the low-symmetry environment.

Subsequent to obtaining assignments for the modes of NiOEC, the observed and calculated vibrational features of NiDMPPh, NiMPPh, and NiPPh were examined and compared with one another and with those of NiOEC. For many RR bands of the pyropheophorbides, the observed frequencies and intensity enhancement patterns allowed a straightforward correlation with modes of NiOEC. The high-frequency modes (above 950 cm^{-1}) of the pyropheophorbides were then plotted in order to assess more critically the effects of further symmetry reduction on the forms of the normal modes and, in particular, to characterize the motions of ring V.

In all cases the vibrational assignments of the nickel(II) dihydroporphyrins were checked for consistency with one another and with the assignments for the parent metalloporphyrin. The criteria included the observed frequencies and intensities as well as the forms of the calculated normal modes. These three criteria were also employed in determining the vibrational assignments for chlorophyll *a* (see Table III). The details of the vibrational assignments for all the molecules are discussed below.

1. NiOEC. a. C_aC_m and C_bC_b Modes. The eight C_aC_m and four C_bC_b stretching vibrations of NiOEC are Raman allowed (4 A and 4 B; 2 A and 2 B, respectively) due to the low symmetry of the molecule. This situation can be contrasted with that which occurs for NiOEP where only four C_aC_m and two C_bC_b modes are RR allowed. On the basis of the spectral analysis and the normal coordinate calculations, the six RR bands of NiOEC observed at 1648 (p), 1644 (ap), 1614 (p), 1590 (ap), 1512 (p), and 1478 (dp) cm^{-1} are attributed to C_aC_m stretching motions, while the three RR bands observed at 1608 (p), 1572, and 1546 (p) cm^{-1} are assigned as C_bC_b stretching motions. The two other C_aC_m modes are predicted to occur between 1460 and 1480 cm^{-1} but are not observed. The fourth C_bC_b stretch involves the reduced pyrrole ring and is calculated at 967 cm^{-1}. This mode is not observed in the RR spectrum. Examination of the IR spectrum of NiOEC (not shown) reveals that several bands are observed near 950 cm^{-1}; however, the spectrum is sufficiently complex in this region to preclude a definitive assignment of the ring IV C_bC_b stretch.[55]

The computed vibrational eigenvectors for the C_aC_m and C_bC_b motions of NiOEC are plotted in Figure 10. Displacements are shown only for those atoms whose motions contribute significantly

(55) Ogoshi, H.; Watanabe, E.; Yoshida, Z.; Kincaid, J.; Nakamoto, K. *Inorg. Chem.* **1975**, *14*, 1344–1350.

Table III. Observed (RR) and Calculated Frequencies (cm^{-1}) of the Fundamental In-Plane Skeletal Modes for NiMPPh, NiPPh, and Chlorophyll *a*

no.	obsd (NiMPPh)	obsd (NiPPh)	obsd (Chl a)[a]	calcd	assignment[b]	corresponding NiOEC modes[c]
1	1700	1700	1690	1704	νCO (V), νC_aC_m (γ)	1
2	1658	1658	1630	1664	νC_aC_m (γ), νCO (V)	1, 2
3		1652 (sh)		1637	νC_aC_m (δ)	1, 2
4				1632	νC_bC_b (III), νC_aC_m (δ)	4, 6
5	1626	1624	1615	1615	νC_aC_m (α, β)	3
6	1604	1604	1560	1570	νC_aC_b (III), νC_bC_b (I)	4, 6, 12
7	1584	1584		1605	νC_aC_m (α, β)	5
8	1574	1574	1530	1573	νC_bC_b (I), νC_aC_b (III)	4, 6, 12
9	1568	1568		1542	νC_bC_b (II), νC_bC_b (I)	7
10				1551	νC_aC_b (II), νC_aC_m (β)	8, 5
11	1524	1522		1515	νC_aC_b (I), νC_aC_b (III)	11, 14
12	1496	1496		1508	νC_aC_b (I), νC_aC_m (γ)	10
13	1482	1484		1493	νC_aC_m (δ), νC_aC_b (I)	9, 14
14				1467	νC_aC_m (α, β), νC_aC_m (δ)	13
15	1452	1454	1440	1485	γCH_2 (V) (scissors), νC_aC_m (γ, δ), νC_aC_b (I, II, III)	12
16	1400	1398	1392	1489	νC_aC_b (II), νC_aC_m (α, δ)	10, 12
17	1396	1392	1381	1386	νC_aN (IV), νC_aC_b (I, III)	15
18	1380	1380	1351	1407	νC_aN (IV), νC_aN (I, III)	16
19	1364	1362	1333	1339	νC_aN (I), δC_mH (δ)	17, 19
20	1350	1356		1306	νC_aN (II), δC_mH (α)	18, 21
21		1338			δCH_2 (vinyl scissors)[d]	
22	1312	1312	1312	1324	νC_aN (II), νC_aN (IV)	15, 18
23	1284	1282	1292	1297	δC_mH (α, β), νC_aN (II, IV)	20
24	1268	1268	1270	1281	δC_mH (α, β)	21
25	1234	1234	1230	1228	δC_bH (IV), δCH_2 (V-9) (wag), δC_mH (δ)	22
26				1229	δC_bH (IV), δC_mH (δ)	23
27				1221	γC_bH (IV), δC_mH (δ)	24
28	1218	1218		1172	δC_bH (IV), νC_aN (IV), δC_mH (δ)	25, 29
29				1207	γC_bH (IV), δC_mH (δ)	26
30	1188	1188	1190	1191	νC_mC_{10} (V), γC_bH (IV)	25, 27
31				1177	δCH_2 (V-10) (twist)	
32	1152	1154	1160	1148	νC_aN (IV), $\delta C_aC_mC_a$ (α, β, γ, δ)	27, 29
33	1132	1134	1149	1073	νC_aN (II), νC_bS, δC_aNC_a (I)	31
34				1129	νC_aC_b (IV), $\delta C_aC_mC_a$ (α, β, γ)	27
35	1122	1122	1115	1109	νC_aC_b (IV), νC_bS	29, 30
36	1100	1100		1080	νC_aC_b (III, IV), νC_aN (I, III)	30
37				1064	νC_aC_m (α), νC_aN (I, II)	32
38				1055	νC_aN (II), δC_mC_aN (II), νC_bS	32
39				1045	νC_aN (III), νC_bS	34
40				1026	$\delta C_mC_aC_b$ (I, II, IV), νC_bS	35
41				1001	νC_aN (III), δC_mC_aN (I)	37
42				989	δC_mC_aN (III), νC_9C_{10} (V)	
43				970	νC_bC_b (IV)	38
					Prominent Modes below 950 cm^{-1}[e]	
44	752	752		715	δC_aC_bS	41
45	658	660		697	δC_aC_bS	44
46	534	526		488	δC_bC_9O	
47		~380			$\delta C_bC_{vinyl(1)}C_{vinyl(2)}$[d]	
48		330		372	δC_aC_bS	45

[a] Data taken from ref 27a. [b] S = C_b substituent. For explanation of other abbreviations and mode descriptors see Table I and Figure 1. [c] The modes of NiOEC which contain similar vibrational motions. Numbers refer to Table I. [d] Vinyl group assignments follow those in ref 58a. [e] Other modes are observed below 950 cm^{-1}; however, the correlation of observed and calculated frequencies is very uncertain due to the high density of calculated modes.

Table IV. Nonfundamental Raman Bands (cm^{-1}) Assignable to In-Plane Skeletal Modes

assignment[a]	NiOEC	NiDMPPh	NiMPPh	NiPPh
$\nu_5 + \nu_{16}$	1764			
$\nu_5 + \nu_9$	1260	1246		
?	1245 (sh)			
$\nu_6 + \nu_8$	1140		1144	
$\nu_{32} + \nu_{35}$	961		~958	960
$2\nu_{35}$	390	388		
$2\nu_{18}$	362	360		

[a] Assignments follow those of ref 28a.

Table V. Correlation of NiOEC Modes Containing Substantial γ,δ-Deformation with Corresponding NiOEC-γ,δ-d_2 Modes[a]

NiOEC		NiOEC-γ,δ-d_2
	A Modes	
1224 (calcd) 1146 (p)	⟶	1186 (p) 946
	B Modes	
1318 (sh) 1227 (calcd) 1107 (calcd)	⟶	1314 (ap) 1212 (calcd) 903 (calcd)[b]

[a] Calcd = calculated mode which is unobserved. [b] The calculated 903 cm^{-1} mode may be observed at 920 cm^{-1}.

to the normal mode (10% or greater of the maximum atomic displacement in a given mode). The calculations indicate that a number of the vibrations, particularly the four highest frequency C_aC_m motions, exhibit a substantial degree of localization into sectors of the macrocycle. The predicted localization phenomenon is substantiated by the results of the deuteriation studies reported here and by those reported by Andersson et al.[24c] Comparison of the RR spectra of NiOEC and NiOEC-γ,δ-d_2 (see Figure 9) shows that the 1648- and the 1644-cm^{-1} bands of NiOEC are both

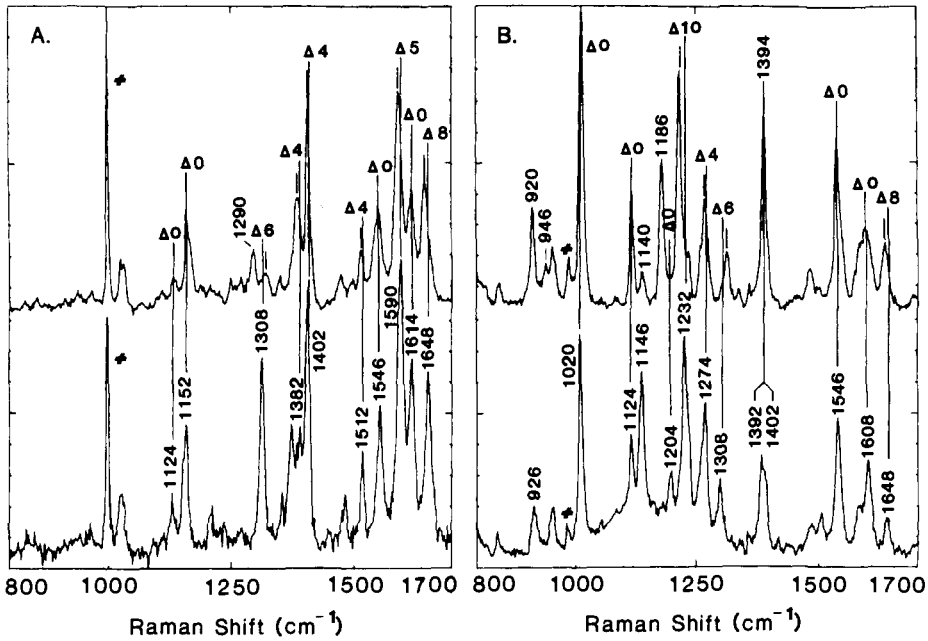

Figure 9. High-frequency region of the RR spectra of NiOEC (bottom) and NiOEC-γ,δ-d_2 (top) obtained with the following: A, Q_x-state excitation (λ_{ex} = 4880 Å); B, Q_y-state excitation (λ_{ex} = 6037 Å). The spectra are of solid samples in Na_2SO_4 pellets, and the internal standard is indicated by the symbol #.

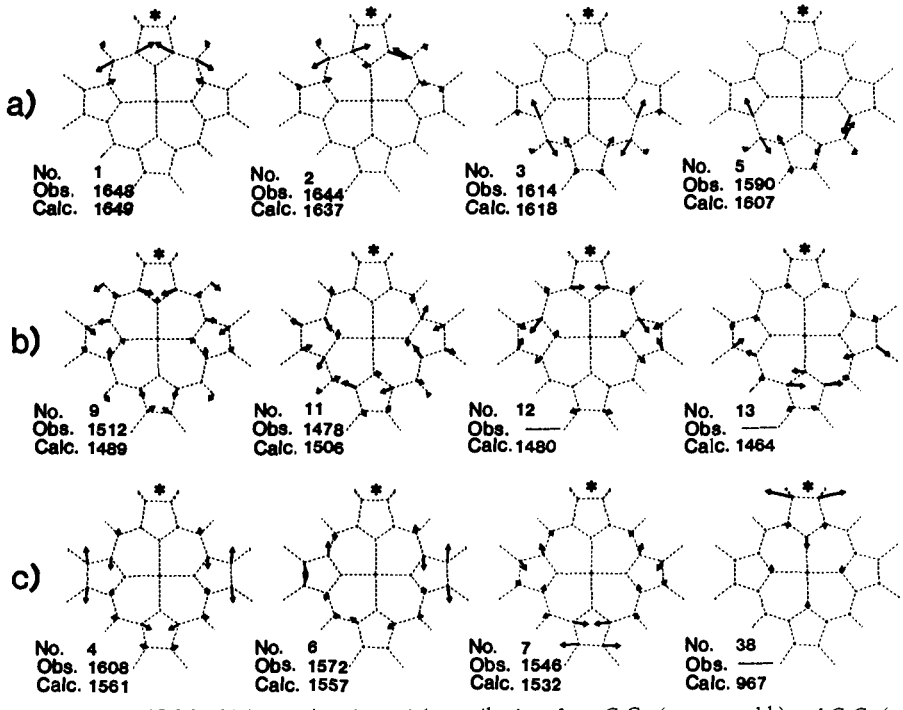

Figure 10. Vibrational eigenvectors of NiOEC which contain substantial contributions from C_aC_m (rows a and b) and C_bC_b (row c) stretching motions. The asterisks denote the reduced pyrrole ring.

down-shifted by approximately 8 cm^{-1} in the deuteriated complex, while the 1614-cm^{-1} band is not shifted at all and the 1590-cm^{-1} band is down-shifted by only 5 cm^{-1}. (It should be noted that the 1644-cm^{-1} band is not clearly observed in the Q_x and Q_y excitation spectra shown in the figure; however, the shift of this band is clear with B-state excitation). On the other hand, RR spectra of copper(II) chlorin and copper(II) chlorin-$\alpha,\beta,\gamma,\delta$-$d_4$ reported by Andersson et al. show that the analogue of the 1648-cm^{-1} band is down-shifted by 9 cm^{-1} in the meso-d_4 vs. the meso-h_4 complex (approximately the same shift as that observed for γ,δ-deuteriation), while the analogues of the 1614- and 1590-cm^{-1} bands are both down-shifted by approximately 15 cm^{-1} (substantially larger shifts than those observed for γ,δ-deuteriation). These deuteriation shifts are in agreement with those predicted by the normal coordinate calculations and are as expected if the motions are partially localized into different sectors of the macrocycle. In particular, the 1648-cm^{-1} mode, which is localized in the γ,δ-methine bridges (see Figure 10), is significantly shifted by deuteriation at these positions but virtually unaffected by additional deuteriation at the α,β-methine positions. Conversely, the 1614- and 1590-cm^{-1} modes, which are localized in the α,β-methine bridges, exhibit exactly the opposite behavior. On the basis of a simple comparison of the RR spectra of NiOEC and NiOEP, it is not possible to predict the localization phenomenon. For example, based on their frequencies and polarization behavior, the 1648- and 1590-cm^{-1} RR bands of NiOEC would appear to be analogues of the RR-allowed ν_{10} (B_{1g}) and ν_{19} (A_{2g}) modes of NiOEP. In addition, the 1644- and 1614-cm^{-1} RR bands of NiOEC could be attributed to RR-active analogues of the IR-allowed ν_{37} (E_u) mode of NiOEP. In actuality, the

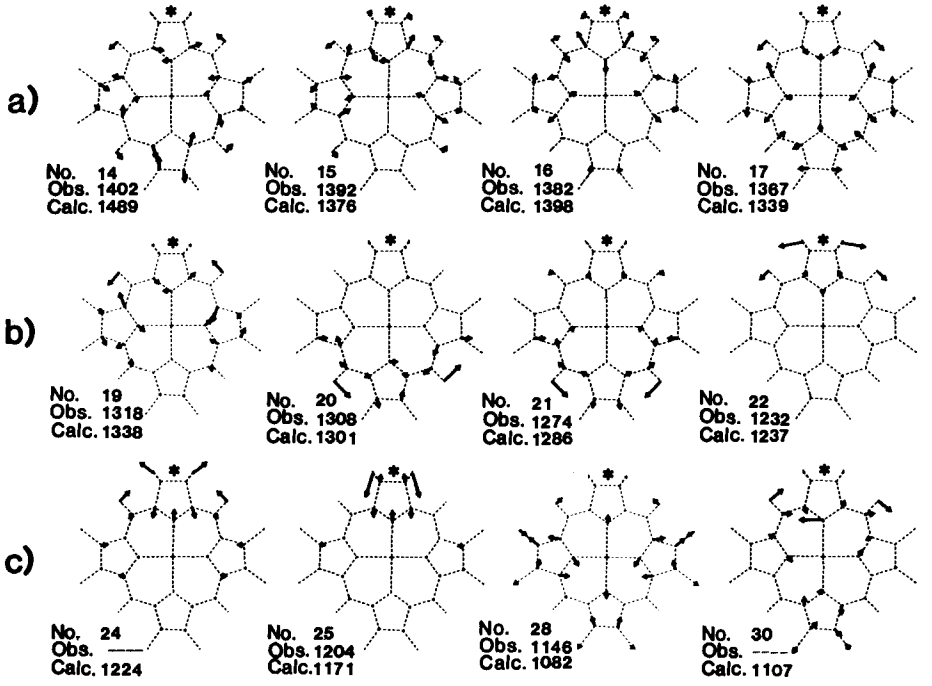

Figure 11. Vibrational eigenvectors of NiOEC which contain substantial contributions from C_aN stretching motions (row a) and CH deformations (rows b and c). The asterisks denote the reduced pyrrole ring. The displacements shown for the substituents on the reduced ring in all cases correspond to C_bH deformations.

normal modes of NiOEC bear little resemblance to those of the parent porphyrin. Instead, the 1648- and 1614-cm^{-1} modes appear to be approximately 50/50 in-phase and out-of-phase linear combinations of ν_{10} and ν_{37a}, whereas the 1644- and 1590-cm^{-1} bands are similar linear combinations of ν_{19} and ν_{37b}.

b. C_aC_b and C_aN Modes. The eight C_aC_b and eight C_aN modes of NiOEC are RR allowed (4 A and 4 B for each mode type). The normal coordinate calculations indicate that these two mode types are mixed extensively with one another and with other skeletal motions and hydrogen-atom deformations (see Table I). Consequently, RR bands which contain substantial contributions from C_aC_b and C_aN stretching motion are scattered throughout the 1000–1400-cm^{-1} spectral region. Four of the most prominent RR bands which can be attributed to C_aC_b and C_aN motions are observed at 1402 (dp), 1392 (ap), 1382 (p), and 1367 (p) cm^{-1}. The calculated vibrational eigenvectors for these four modes are shown in Figure 11 (row a). As can be seen, these modes do not exhibit any significant degree of localization into sectors of the macrocycle. The same is true for the remaining C_aC_b and C_aN modes (not shown).

The two polarized RR bands of NiOEC at 1382 and 1367 cm^{-1} are of particular interest. The RR spectra of all metallochlorins examined to date exhibit analogues of these two bands.[3,4,6,24] The RR spectra of 2,4-diacetyl- and 2,4-diformyl-substituted nickel(II) porphyrins also display two bands in this region.[54] The symmetry of these porphyrins is substantially lower than D_{4h} owing to the presence of the two conjugating groups.[56] The two polarized RR bands of metallochlorins are both sensitive to ^{15}N substitution[21a] and are at frequencies similar to that of the ν_4 (A_{1g}) mode of metalloporphyrins.[28] Our calculations accurately reproduce the 5–6-cm^{-1} isotope shifts observed for both of these bands in CuOEC-$^{15}N_4$.[21a] Comparison of the vibrational eigenvectors calculated for these modes (Figure 11) with those calculated for NiOEP indicates that the two chlorin modes are derived from ν_4 and ν_{41a} (E_u). However, due to mixing, neither of the NiOEC modes can be exclusively described as an analogue of one or the other of the parent porphyrin modes.

c. In-Plane C_mH and C_bH Modes. All four in-plane C_mH modes are RR allowed for NiOEC (2 A and 2 B). In addition, the two in-plane deformations corresponding to C_bH motions on ring IV are RR allowed (A and B—it should be noted that the distinction between in-plane and out-of-plane motions is only approximate because ring IV is twisted[47]). The C_bH modes would not be expected to exhibit RR intensity if they are assumed to be isolated from vibrations involving atoms along the π-conjugation pathway. However, this assumption is not borne out by the spectral data as will be discussed below.

The RR spectrum of NiOEC exhibits relatively intense bands at 1308 (ap), 1274 (p), 1232 (p), and 1204 (p) cm^{-1} which would seem to be candidates for the C_mH deformations based on analogy to NiOEP (see Figure 5). However, three of the modes are symmetric, whereas only two symmetric C_mH vibrations are expected. In addition, the pyropheophorbides exhibit a four-banded RR pattern in this spectral region similar to that observed for NiOEC despite the fact that these five-ring molecules contain only three meso hydrogens. The normal coordinate calculations provide an explanation for these observations. Specifically, the calculations indicate that both the α,β- and γ,δ-hydrogen motions of NiOEC are mixed with porphyrin skeletal modes, and, in addition, the latter motions are mixed with the C_bH deformations on ring IV. As a consequence, the γ,δ-motion is dispersed among a number of vibrations, and the assignment of a single RR band to a particular γ,δ-deformation is an oversimplification.

Eight modes which are predicted to contain a significant amount of C_mH and/or C_bH motion are shown in Figure 11 (rows b and c). The calculations suggest that the 1308- and 1274-cm^{-1} RR bands are due to modes which primarily involve localized deformation of the α,β-hydrogens. This assignment is confirmed by the observed (see Figure 9) and calculated deuteriation shifts for NiOEC-γ,δ-d_2. In particular, both the 1308- and 1274-cm^{-1} bands are quite insensitive to γ,δ-deuteriation with observed (calculated) shifts of +6 cm^{-1} (+2 cm^{-1}) and −4 cm^{-1} (−6 cm^{-1}), respectively. Nevertheless, the intensities of the RR bands associated with the antisymmetric α,β-deformation are quite different for the protonated (1308 cm^{-1}) and γ,δ-deuteriated (1314 cm^{-1}) species. This intensity difference is probably due to different degrees of mixing of this motion with other motions in the excited electronic states of the two complexes. In this context, a nearby antisymmetric mode (1318 cm^{-1} in the protonated complex) also appears to change its RR intensity upon deuteriation (1290 cm^{-1}).

As was previously noted, the assignment of the γ,δ-hydrogen deformations is extremely difficult due to the distribution of this

(56) Bocian, D. F.; Masthay, M. B.; Birge, R. R. *Chem. Phys. Lett.* **1986**, *125*, 467–472.

motion into a number of eigenvectors (see Figure 11). The deuteriation experiments provide insight into the complicated nature of these hydrogen deformations. The RR spectrum of NiOEC-γ,δ-d_2 exhibits a weak band at 946 cm^{-1} (and possibly a band at 920 cm^{-1}) which is (are) assignable to γ,δ-deuteron motion. However, none of the modes at higher frequency, with the exception of the 1146-cm^{-1} band which appears to up-shift to 1186 cm^{-1}, are significantly altered by γ,δ-deuteriation. These results indicate that a simple, one-to-one correlation of the RR spectral features of NiOEC and NiOEC-γ,δ-d_2 is not possible.

The complicated spectral changes which occur upon γ,δ-deuteriation of NiOEC led us to reexamine the spectral data and calculated normal coordinate descriptions of NiOEP and NiOEP-d_4. It was found that difficulties are also experienced in making one-to-one correlations of isotopically shifted bands of the deuteriated complex with those of the parent porphyrin. These difficulties are made evident by a comparison of the results for NiOEP reported by Abe et al.[28b] with those reported by Gladkov and Solovyov.[43c] These two groups predict different eigenvectors and, hence, different deuteriation shifts for both the A_{2g} and B_{1g} C_mH deformations of the complex. For example, the Japanese workers predict that meso deuteriation shifts the A_{2g} modes at 1308 (ν_{21}) and 1121 (ν_{22}) cm^{-1} to 890 and 1202 cm^{-1}, respectively, whereas the Soviet workers interchange these shifts. A similar interchange of spectral assignments is made for the two B_{1g} modes. Careful examination of the normal mode descriptions of NiOEP and NiOEP-d_4 indicates that neither of the above interpretations of the deuteriation shifts is correct. In fact, all four modes contain C_mH character, and deuteriation leads to extensive mixing of the two original eigenvectors in a given symmetry block. Consequently, the deuteriation shifts can only be considered collectively rather than individually (a many-to-many vs. a one-to-one mapping). Taking this fact into consideration, the different deuteriation shifts reported for the C_mH modes of NiOEP by the Japanese and Soviet groups are interpretive rather than substantive in nature.

The complications which arise in the interpretation of the isotopic substitution data for NiOEP are carried over to NiOEC but are exacerbated by the participation of the C_bH motions. In this regard, the normal coordinate calculations predict that the symmetric mode containing the most γ,δ-hydrogen character occurs at 1224 cm^{-1} (see Figure 11) and is apparently unobserved. The eigenvector of this vibration and that of the 1146-cm^{-1} mode, which also contains γ,δ-character, are mixed upon deuteriation. The two resulting modes are observed at 1186 and 946 cm^{-1}. In the case of the antisymmetric γ,δ-hydrogen deformation, the calculations indicate that the mode with the largest amount of this motion occurs at 1107 cm^{-1} but, like its symmetric counterpart, is apparently unobserved. The eigenvector of this vibration is mixed with those of several other modes upon deuteriation. These include the observed mode at 1318 cm^{-1} and a calculated mode at 1227 cm^{-1}. The vibrations which result from the redistribution of these eigenvectors upon deuteriation include the observed mode at 1290 cm^{-1} (and possibly the mode at 920 cm^{-1}) and a calculated mode at 1212 cm^{-1}. These correlations are summarized in Table V. It is interesting to note that the description of the α,β-hydrogen modes of NiOEC, which are isolated from the γ,δ-deformations, is simpler than that of the hydrogen deformations of NiOEP. For the chlorin, only one mode of each symmetry type (A and B) contains a significant amount of α,β-hydrogen deformation; for the porphyrin, several modes in each pertinent symmetry block (two A_{2g}, two B_{1g} and three E_u) contain substantial amounts of C_mH motion.

The observed and calculated frequencies and γ,δ-deuteriation shifts of the 1232- and 1204-cm^{-1} modes of NiOEC strongly suggest that these bands are due to vibrations which contain a substantial amount of C_bH deformation. It seems highly unlikely that both of these intense RR bands could be due to combinations or overtones. The assignment of these modes to C_bH deformations is supported by the fact that similar features are observed in the RR spectra of the five-ring molecules. These modes could gain RR intensity via mixing with vibrations of the porphyrin skeleton, although the calculated vibrational eigenvectors do not exhibit an extensive amount of skeletal motion. However, the RR intensities are determined by the origin shift of the excited electronic state relative to the ground state. Conformational changes could occur around ring IV in the electronic excited state which could result in substantial origin shifts for the C_bH deformations.

d. Other Modes. A number of the RR bands of NiOEC which have not been heretofore discussed exhibit frequencies similar to those of modes in the spectra of NiOEP. Certain of these NiOEP modes have been assigned as fundamentals which primarily involve motions of the C_b-ethyl groups while others have been attributed to combination and overtone vibrations. The normal coordinate calculations predict that the frequencies of the C_b-ethyl motions of NiOEC are similar to those of NiOEP. Consequently, assignments for these RR bands and those attributed to nonfundamentals were made by analogy to previous studies of NiOEP.[28]

2. NiDMPPh, NiMPPh, and NiPPh. a. C_aC_m and C_bC_b Modes. The RR spectra of NiDMPPh, NiMPPh, and NiPPh differ most dramatically from those of NiOEC in the 1500–1700-cm^{-1} spectral region (see Figures 3–5), where vibrations associated with C_aC_m and C_bC_b bond stretches are observed. Vibrations due to these types of motion might be expected to be those most perturbed by the addition of the isocyclic ring because a C–C bond replaces a C–H bond at the γ-methine position, and substantial strain is placed on the skeletal bonds in the region of ring V.[48,49] The result is an up-shift in the frequencies of three of the four highest energy C_aC_m stretches and two of the three high-energy C_bC_b stretches relative to those of the analogous modes of NiOEC. For example, C_aC_m stretching modes are observed at 1658, 1652, 1626, and 1584 cm^{-1} in NiPPh compared with 1648, 1644, 1614, and 1590 cm^{-1} in NiOEC (see Tables I and III). The other four C_aC_m modes are also affected by the presence of the fifth ring. These vibrations are mixed with the C_aC_b modes to a greater degree than in NiOEC, and it is not accurate to classify them exclusively as C_aC_m motions. As would be anticipated, the C_bC_b stretching mode on the reduced ring is essentially unaffected by the presence of the isocyclic ring.

The computed vibrational eigenvectors for the four highest energy C_aC_m stretches and the four C_bC_b stretches of NiMPPh are shown in Figure 12 (rows a and b, respectively). In the case of the C_aC_m stretches, the localization into sectors of the macrocycle which occurs in NiOEC persists after addition of the isocyclic ring. However, the eigenvectors of the two vibrations of NiMPPh which are localized in the methine bridges adjacent to ring IV bear little resemblance to those of the analogous modes of the basic chlorin. Instead, these modes appear to be linear combinations of the two NiOEC vibrations. This results in further localization of these two C_aC_m modes of the pyropheophorbide into motions primarily involving either the γ- or δ-methine bridges. In contrast, the eigenvectors of the two vibrations of NiMPPh which are localized in the methine bridges adjacent to ring II appear to be quite similar to those of NiOEC. Comparison of the three high-frequency C_bC_b modes of NiMPPh with those of NiOEC (cf. Figures 12 and 10) reveals that the addition of the isocyclic ring also results in a significant redistribution of the eigenvectors of these modes. Specifically, the C_bC_b stretch of each inequivalent pyrrole ring of NiMPPh is relegated to a separate mode. In addition, these modes contain contributions from C_aC_m stretches and the C_aC_b stretch of ring III. Examination of the eigenvectors for the C_aC_m and high-energy C_bC_b stretches of NiDMPPh (not shown) indicates that these modes are also redistributed relative to those of NiOEC. However, comparison of the eigenvectors of NiDMPPh with those of NiMPPh clearly indicates that the presence of the C_9 carbonyl group is important for determining the exact forms of the normal coordinates. As can be seen in Figure 12, the carbonyl stretching mode mixes with certain of the C_aC_m and C_bC_b vibrations. In addition, the strain in the macrocycle is altered by the presence of the CO group. Although the isocyclic ring and keto group significantly perturb the eigenvectors of the C_aC_m and C_bC_b modes of the five-ring complexes relative to those of NiOEC, we have attempted to correlate the modes of the pyropheophorbides with those of the

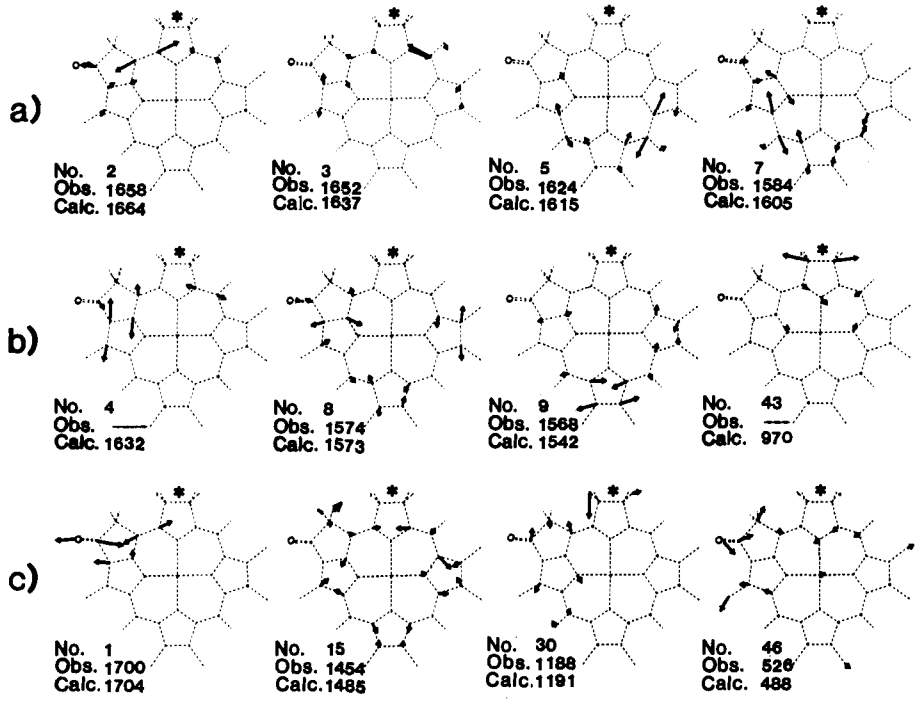

Figure 12. Vibrational eigenvectors of NiMPPh which contain substantial contributions from C_aC_m (row a) and C_bC_b (row b) stretching motions and from ring V motions (row c). The asterisks denote the reduced pyrrole ring.

parent chlorin. These correlations are summarized in Tables II and III.

b. Other Skeletal Modes. The RR spectra of the five-ring molecules in the spectral region below 1500 cm^{-1} are in general quite similar to those of NiOEC. This observation indicates that bands due to γ,δ-C_mH deformations are not clearly manifested in the RR spectra of the pyropheophorbides and is consistent with our characterization of the RR spectra of NiOEC. The normal coordinate calculations for NiDMPPh and NiMPPh predict that many of the eigenvectors for the modes below 1500 cm^{-1} bear a strong resemblance to those of NiOEC. This is reflected in the greater incidence of one-to-one correlations of modes of the pyropheophorbides with those of the parent chlorin (see Tables II and III).

c. Ring V Modes. Bands are observed in the RR spectra of NiDMPPh, NiMPPh, and NiPPh which have no apparent analogues in the spectra of NiOEC. On the basis of the spectral comparisons and the normal coordinate calculations, we have assigned some of these bands to vibrations of ring V (see Tables II and III). The C_9 carbonyl stretching vibration is observed near 1700 cm^{-1} for NiMPPh and NiPPh. This mode has been previously identified in the RR spectra of various chlorophylls.[27] In addition, a band is observed near 530 cm^{-1} for these two complexes which is absent from the spectra of NiDMPPh. We tentatively assign this band to the in-plane carbonyl deformation.[57] All three pyropheophorbides exhibit a band in the 1180–1190-cm^{-1} spectral region which we attribute to the C_mC_{10} stretching vibration. The calculated vibrational eigenvectors for this mode and the two carbonyl modes of NiMPPh are shown in Figure 12 (row c). As is evident, all three of these modes contain substantial contributions from in-plane deformations of the macrocycle.

It is of particular interest that the B-state excitation RR spectra of NiDMPPh exhibit two bands at 1438 and 1424 cm^{-1} while only a single corresponding band is observed near 1450 cm^{-1} in the spectra of NiMPPh and NiPPh. The normal coordinate calculations suggest that these bands may be due to the CH_2 scissoring motions on ring V. The eigenvector calculated for the single scissoring vibration of NiMPPh is pictured in Figure 12 (row c). As can be seen, the normal coordinate for this nominally out-of-plane vibration contains a large amount of in-plane skeletal motion. This mixing could be responsible for the RR intensity of the mode.

d. Vinyl Modes. The NiPPh complex differs from the other nickel(II) dihydroporphyrin complexes examined here in that it contains a vinyl substituent at the 2-position (ring I). The effects of this group on the RR spectra are evident upon comparison of the results for NiPPh with those for NiMPPh. Specifically, the band at 1338 cm^{-1} in the spectra of NiPPh has no apparent analogue in the spectra of NiMPPh. Although this band is rather intense, we attribute it to the vinyl CH_2 scissoring motion based on analogy to the results obtained for porphyrins by Choi et al.[58] Another apparent effect of the vinyl group is evident in the difference in the intensities of the RR bands near 1130 cm^{-1} in the spectra of the two complexes. Porphyrin vibrations in this region have previously been reported to contain contributions from C_b-vinyl stretching motion, and similar contributions might be expected for chlorins. One other feature in the RR spectra of NiPPh which may be caused by the vinyl substituent is observed with Q_y excitation. Two peaks near 380 cm^{-1} are well-resolved in the spectra of NiMPPh but appear to be obscured by a third feature in the spectra of NiPPh. We tentatively attribute this third mode to a $C_bC_{vinyl(1)}C_{vinyl(2)}$ angle-bending motion, again, based on analogy to the results of Choi et al.[58] Finally, there is no evidence of strong RR activity for the $C_{vinyl(1)}C_{vinyl(2)}$ stretching motion upon excitation in any region of the absorption spectrum. This is consistent with the results reported for chlorophylls by Lutz and co-workers.[27]

3. Chlorophyll *a*. The most important difference between the metallodihydroporphyrins we examined and chlorophyll *a* is the metal center. The change of the metal ion from Ni(II) to Mg(II) has a substantial effect on the core size and, hence, certain vibrational frequencies.[19,20,51] The presence of the carbomethoxy group at the C_{10}-position of chlorophyll *a* has some influence on the RR spectrum, although the effect is not observed to be large.[59] As a consequence of the larger metal ion, the C_aC_m, C_bC_b, and C_aN stretching modes are shifted to lower frequencies by approximately 20–30 cm^{-1}. However, the RR intensity pattern of chlorophyll *a* is comparable to that of the NiMPPh and NiPPh

(57) Kartha, V. B.; Mantsch, H. H.; Jones, R. N. *Can. J. Chem.* **1973**, *51*, 1749–1766.

(58) (a) Choi, S.; Spiro, T. G.; Langry, K. C.; Smith, K. M. *J. Am. Chem. Soc.* **1982**, *104*, 4337–4344. (b) Choi, S.; Spiro, T. G.; Langry, K. C.; Smith, K. M.; Budd, D. L.; LaMar, G. N. *Ibid.* **1982**, *104*, 4345–4351.

(59) Andersson, L. A., private communication.

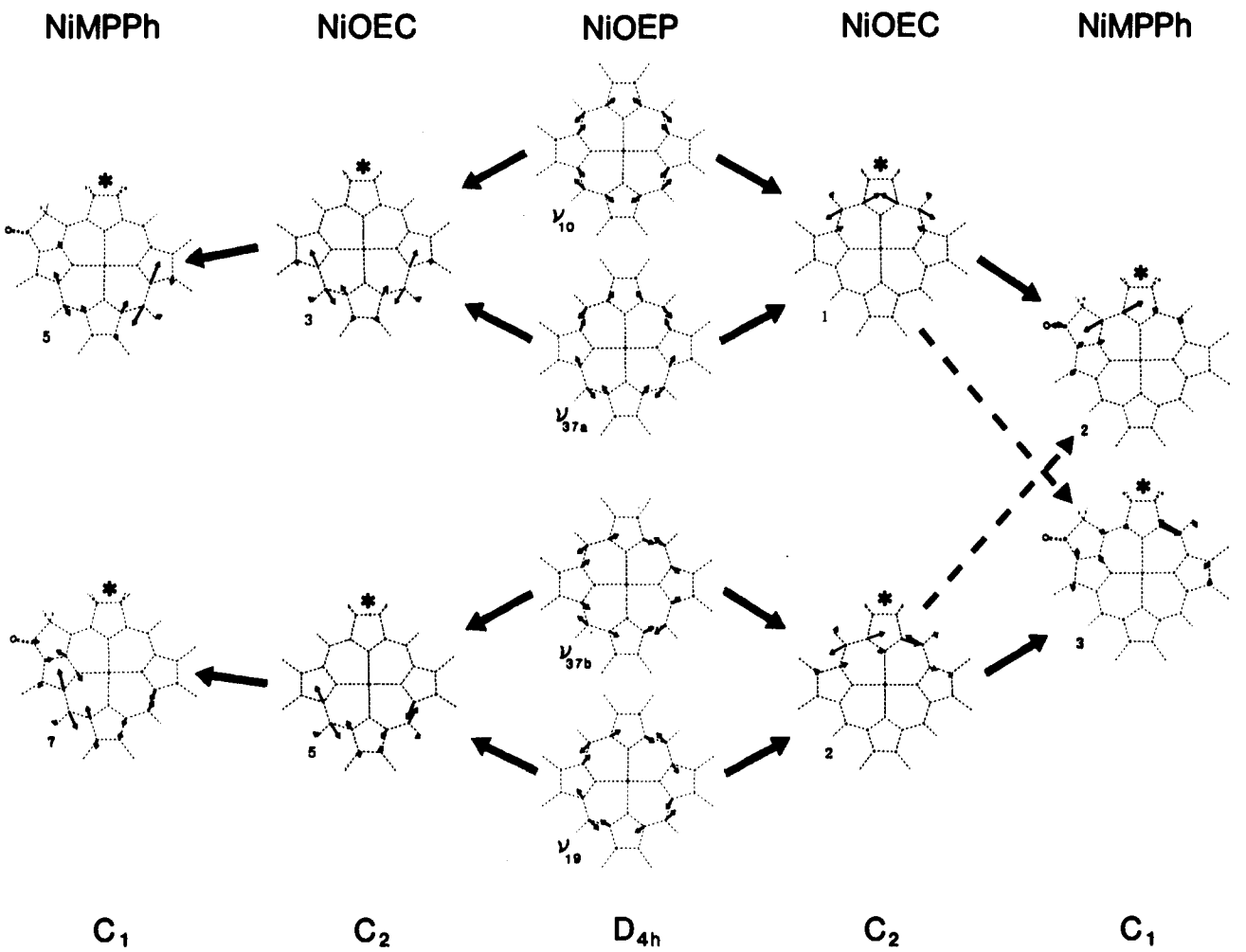

Figure 13. Effects of decending symmetry on the high-frequency C_aC_m stretching motions of the porphinato-macrocycle.

which suggests that the normal coordinate descriptions for the natural pigment are similar to those of the Ni(II) complexes. It is noteworthy that the observed frequencies for chlorophyll *a* in the 1150–1350-cm^{-1} spectral region are essentially identical with those observed for NiMPPh and NiPPh. This lends further credence to our assignment of bands in this region to hydrogen deformations and ring V modes.

B. Effects of Low-Symmetry on the Electronic and Vibrational Structure. The reduction of one of the pyrrole rings of a metalloporphyrin has a dramatic effect on the electronic properties of the molecule.[13b] The degenerate B and Q electronic excited states of the tetrapyrrole system are split, and the oscillator strengths for the two members of the split pair become unequal. The effects are most dramatic in the Q state where the splittings can be as large as 2000–3000 cm^{-1}, and the oscillator strengths can differ by a factor of ten. The additional structural features endogenous to natural photosynthetic pigments (isocyclic ring, 9-keto group, and 2-vinyl group) further increase the inequivalence of the Q_x and Q_y states (see Figure 2). The changes in the electronic structure which result from pyrrole-ring reduction and the addition of peripheral groups have strong effects on the vibrational frequencies, intensities and normal mode descriptions. The effects on the latter two properties are the most profound.

The results of the RR studies reported here reflect the complicated nature of the effects of low symmetry on the electronic and vibrational properties of metallodihydroporphyrins. The changes in the electronic structure of the molecule are manifested in the behavior of the RR intensities as a function of the excitation wavelength. Detailed RR excitation profiles have not yet been reported for any metallodihydroporphyrins, and it is not possible to determine exactly how the descent in symmetry alters the electronic excited-state displacements and the vibronic coupling mechanisms of the metallochlorins relative to the metalloporphyrins. Nevertheless, the RR studies reported here lend some insight into the effects of the low-symmetry environment on these properties. Specifically, the RR spectra of NiOEC obtained with Q_y excitation exhibit symmetric modes which are predominantly derived from the B_{1g} modes of metalloporphyrins, whereas the spectra obtained with B excitation exhibit symmetric modes which are predominantly derived from the A_{1g} modes. This observation indicates that the Franck–Condon factors for the symmetric vibrations are quite different between the Q_y and B electronic excited states. The enhancement of the B_{1g}-derived modes of the chlorins with Q_y-state excitation suggests that the origin shifts along these normal coordinates might be qualitatively viewed as originating from distortions similar to the Jahn–Teller displacements experienced by the higher symmetry porphyrins.[60] Furthermore, the enhancement behavior of the A_{1g}-derived modes of the chlorins suggests that the nature of the origin shifts of these modes could be similar to those of the parent porphyrin. The observation that the asymmetric modes of NiOEC exhibit RR intensity with excitation in both the Q_x and Q_y states indicates that a Herzberg–Teller scattering mechanism is operative for these states.[17-20] The fact that the RR enhancements of the asymmetric modes are approximately equal for Q_x and Q_y excitation suggests that the Q_x state is vibronically coupled to the Q_y state in addition to the B state. If this were not the case, the Q_x scattering intensity would be substantively less than the Q_y intensity due to the lower oscillator strength of the Q_x state. It should be noted that the proximity of the Q_x state to the B state is not sufficient to account for the equal RR intensities of the asymmetric modes observed with Q_x and Q_y excitation (presuming $\partial H/\partial Q$ is the same for a

(60) (a) Shelnutt, J. A.; Cheung, L. D.; Chang, R. C. C.; Yu, N.-T.; Felton, R. H. *J. Chem. Phys.* **1977**, *66*, 3387–3398. (b) Shelnutt, J. A. *J. Chem. Phys.* **1981**, *74*, 6644–6656.

given mode in the two states). To gain additional insight into the scattering mechanisms for metallochlorins, we are acquiring detailed RR excitation profiles throughout the red and blue regions of the absorption spectrum.

The perturbation of the electronic structure which occurs in the low-symmetry environment of the metallochlorins substantially alters the forms of the vibrational eigenvectors relative to those of metalloporphyrins. The most interesting effect is the localization of certain modes into semicircles or quadrants of the macrocycle. The localization phenomenon is most dramatic for the highest frequency C_aC_m stretching vibrations. These modes of NiOEC appear to be 50/50 in-phase and out-of-phase linear combinations of pairs of NiOEP modes whereas certain of the C_aC_m modes of the pyropheophorbides appear to be linear combinations of pairs of NiOEC modes. This is illustrated in Figure 13 which depicts the effects of the descending symmetry on the vibrational eigenvectors of the C_aC_m stretches. The eigenvectors plotted on the right (left) side of the figure illustrate the in-phase (out-of-phase) linear combinations of the modes of the higher symmetry parent group.

The vibrational localization which occurs in the metallodihydroporphyrins can be rationalized in terms of the geometrical structure of the molecules. For metallo-OEC complexes, the methine bonds alternate in length (short-long-short-long, beginning from the reduced pyrrole ring).[45-47] This in turn alters the values of the force constants for the bonds. The C_aC_m stretches of adjacent methine bonds remain strongly coupled because the off-diagonal **F**-matrix element which couples these two stretches is sizable relative to the difference in the diagonal **F**-matrix elements for the two bonds. In contrast, the off-diagonal **F**-matrix element which couples the pairs of C_aC_m stretches separated by either pyrrole rings I or III is small relative to the difference in the diagonal **F**-matrix element for the C_aC_m bonds on opposite sides of the intervening pyrrole. As the difference between these two diagonal **F**-matrix elements becomes larger, the localization of the vibrational modes on either side of the rings I and III becomes more pronounced. This does not occur for modes which contain large amounts of C_aC_b and C_aN motion (which includes the four lowest frequency C_aC_m stretches) because the C_aC_b and C_aN bonds do not exhibit length alternation. Upon addition of the isocyclic ring, the diagonal **F**-matrix elements for the C_aC_m bonds on opposite sides of rings II and IV are no longer equivalent by symmetry. This results in localization of the C_aC_m stretches into quadrants of the macrocycle, especially in the reduced pyrrole section of the ring. This type of localization phenomenon should be a general feature of large molecules in which the intrinsic force constants for nearby bonds are substantially different.

C. Implications of Low-Symmetry for Interchromophore Interactions in Photosynthetic Aggregates. The electronic properties which are imparted to metallochlorins due to the low symmetry of the molecules most probably have a significant impact on the efficiency of photosynthetic units. The large oscillator strength of the Q_y state of chlorophyll provides a means of increasing the amount of interchromophore coupling in dimeric and larger aggregates of photosynthetic pigments over that which would be possible in organized collections of higher symmetry metalloporphyrins. This property of chlorophyll can be put to the most efficient use in systems such as photosynthetic reaction centers because the chromophores in these proteins are held rigidly in specific orientations with respect to one another.[61] It is interesting to speculate whether the normal mode localization which occurs in the metallochlorins is important for further enhancing the amount of interchromophore coupling in photosynthetic aggregates. It is conceivable that the vibronic interaction between the two chlorophyll molecules which comprise the special pair could be increased significantly by the spatial overlap of portions of the molecules in which localized vibrational motions occur. Examination of the crystallographic data for the reaction center protein obtained from the photosynthetic baterium *Rhodopseudomonas viridis*,[62] which contains bacteriochlorophyll *b*, suggests that the geometrical arrangement of the special pair could facilitate the overlap of localized vibrational modes. It remains to be determined whether such overlap has any significant impact on the efficiency of interchromophore interactions and charge separation.

Acknowledgment. This work was supported by Grants GM-36243 (D.F.B.) and GM-34548 (R.R.B.) from the National Institutes of Health. D.F.B. also acknowledges support from the Alfred P. Sloan Foundation (1982-1986). We thank Drs. L. A. Andersson and T. M. Loehr for communicating their results prior to publication.

(61) Boxer, S. G. *Biochim. Biophys. Acta* **1983**, *726*, 265-292.
(62) (a) Deisenhofer, J.; Epp, O.; Miki, K.; Huber, R.; Michel, H. *Nature (London)* **1985**, *318*, 618-624. (b) Deisenhofer, J.; Michel, H.; Huber, R. *Trends Bio. Sci.* **1985**, *10*, 243-248. (c) Deisenhofer, J.; Epp, O.; Miki, K.; Huber, R.; Michel, H. *J. Mol. Biol.* **1984**, *180*, 385-398.